Published in final edited form as:

Pflugers Arch. 2021 September ; 473(9): 1517–1537. doi:10.1007/s00424-021-02564-9.

Structure and dynamics of photoreceptor sensory cilia

Theodore G. Wensel[1], **Valencia L. Potter**[1,2], **Abigail Moye**[3], **Zhixian Zhang**[3], **Michael A. Robichaux**[4]

[1]Vera and Marrs McLean Department of Biochemistry and Molecular Biology and Developmental Biology Graduate Program, Baylor College of Medicine, Houston, TX 77030, USA

[2]Medical Scientist Training Program (MSTP), Baylor College of Medicine, Houston, TX 77030, USA

[3]Vera and Marrs McLean Department of Biochemistry and Molecular Biology, Baylor College of Medicine, Houston, TX 77030, USA

[4]Departments of Ophthalmology and Biochemistry, West Virginia University, Morgantown, WV, USA

Abstract

The rod and cone photoreceptor cells of the vertebrate retina have highly specialized structures that enable them to carry out their function of light detection over a broad range of illumination intensities with optimized spatial and temporal resolution. Most prominent are their unusually large sensory cilia, consisting of outer segments packed with photosensitive disc membranes, a connecting cilium with many features reminiscent of the primary cilium transition zone, and a pair of centrioles forming a basal body which serves as the platform upon which the ciliary axoneme is assembled. These structures form a highway through which an enormous flux of material moves on a daily basis to sustain the continual turnover of outer segment discs and the energetic demands of phototransduction. After decades of study, the details of the fine structure and distribution of molecular components of these structures are still incompletely understood, but recent advances in cellular imaging techniques and animal models of inherited ciliary defects are yielding important new insights. This knowledge informs our understanding both of the mechanisms of trafficking and assembly and of the pathophysiological mechanisms of human blinding ciliopathies.

Keywords

Photoreceptors; rods; cones; primary cilia; ciliopathies; cytoskeleton; electron microscopy; superresolution fluorescence; retina

Correspondence to TGW: twensel@bcm.edu.

Conflicts of interests/Competing interests: The authors declare no conflicts of interest or competing interests.

Code availability: Not applicable

Introduction

Rod and cone photoreceptors of the vertebrate retina have evolved highly specialized structures that are uniquely optimized to serve their functions of light detection over a very wide range of light intensities, with maximal temporal, spatial and wavelength resolution for each intensity range. They have adapted a structure found in diverse cell types in virtually all metazoan species, the sensory cilium, or primary cilium, into an enlarged photo-sensing organelle, the photoreceptor sensory cilium, which serves as an incredibly efficient detector and transducer of visual signals, macromolecules, and membranes (see quantitative estimates below).

Cilia in most eukaryotic cells are tiny, hair-like organelles built around a central core of microtubules, surrounded by a thin layer of cytoplasm and a ciliary membrane of unique composition. These protruding organelles are often referred to as “signaling hubs” and are involved in diverse functional roles, including sensation of the external environment (olfactory and photoreceptor cells), fluid movement (trachea, brain, and the embryonic node), and in signaling pathways like Sonic Hedgehog. They are present in most cell types in metazoan organisms at some stage in the cell cycle and share the defining feature of a central bundle of microtubules. They are broadly classed into two types. Motile cilia possess a 9+2 microtubule architecture, along with additional structures such as dynein arms and “central spokes” needed for motility. Immotile cilia, also known as primary or sensory cilia, possess a 9+0 microtubule architecture at their base and lack the central pair of microtubules and the additional motility-related structures. The photoreceptor sensory cilia (Fig. 1) belong to this non-motile class. They differ from most other primary cilia in having large disc membranes, on which phototransduction takes place, extending from the ciliary microtubules in a highly specialized compartment of the cell called the outer segment (OS). The OS is connected to the inner segment (IS), where most biosynthesis takes place, by a thin section, known as the connecting cilium (CC), which contains no discs, has a bundle of 9 microtubule doublets, and serves as a conduit through which large amounts of proteins, membranes and small molecules must continually flow (see quantitative estimates below). There are many attributes that make the photoreceptor cilium unique. In this review we briefly summarize our current understanding of the structure and dynamics of this complex network of molecular machines and highlight some of the current areas of active research interest.

Methods for determination of cilium-associated structures.

Because of their small size, cilia in general, and the CC of the photoreceptor sensory cilia in particular, pose daunting challenges for structural analysis. In the first several decades of research on photoreceptor structure, the most widely-used tool was conventional transmission electron microscopy (TEM) of fixed, embedded and sectioned retina (see multiple references in [214] and examples below), with contrast provided by heavy-metal stains.

Scanning electron microscopy (SEM) of metal-coated surface structures and freeze-fractured membranes also played an important role [158–160] (Fig. 2). The high contrast and high

resolution of conventional TEM, capable in the best images (but far from routinely) of resolving individual tubulin protofilaments at a spacing of 5.5 nm, is achieved at the expense of harsh fixatives, dehydration and heavy metal stains that can distort some structural features, obscure others, and give rise to contrast by uncertain mechanisms that complicate interpretation. Translation of two-dimensional projection images into three dimensional structures has traditionally required extremely laborious serial sectioning and reconstruction, but automation-based pipelines and instruments developed in recent years have led to increases in speed, accuracy, and resolution of such reconstructions. A combination of serial sectioning with electron tomography, in which each section is imaged over a range of tilt angles, can be used to generate three-dimensional maps of relatively large volumes, on the order of a few cubic micrometers. This approach has been applied successfully to the basal discs of rod OS [204,19] (see Fig. 3) and to sensory cilia of epithelial cells [189]. High pressure freezing and freeze-substitution prior to embedding can help to preserve structural integrity in 3D TEM, as well as eliminate artifacts caused by harsh fixatives [205].

In recent years cryo-electron tomography (cryo-ET) has emerged as an increasingly powerful technique for determining details of cellular ultrastructure [115,100,116,6,51,141], including structures of cilia and adjacent features in ciliated cells. It has the advantage of preserving sample integrity in vitreous ice without chemical fixation or heavy-metal stains, and scattering intensity reflects the mass of the underlying biological features rather than heavy metals forming contrast by being excluded from or adhering to those structures. This technique has been used extensively on motile cilia [137,187,43,135,10,69,151,18,139,86,144,63,97], which are larger and structurally more robust and rigid than primary cilia, and can be readily isolated to allow averaging of images of large numbers of motile cilia. Among the first applications of cryo-electron tomography to primary cilia were studies of vertebrate photoreceptor sensory cilia [129,58,213,138,157]. Early cryo-tomograms of rod cilia were quite noisy and had resolutions limited to tens of nanometers. However, over the last decade or so improved instrumentation has become available, including more sensitive direct electron detectors, higher accelerating voltages for thicker samples, energy filters and improved sample loading and imaging automation. These improvements, together with advances in software to allow rapid subtomogram averaging driven by machine learning algorithms (Fig. 4) have opened the way to obtaining structures at nanometer and sub-nanometer scales [157,168,172,235,165,232,207,12,49,24,32,48,104].

An intrinsic limitation on the application of cryo-ET to retinal samples is the requirement for the sample to be no more than a few hundred nm in thickness, and to be of low enough mass to be susceptible to freezing in a few milliseconds upon being plunged into a cryogenic fluid. This problem has in the past been overcome by the use of isolated rod cells, but these are necessarily fragments of the cells, separated from their native environment, and subject to distortions such as flattening or membrane vesiculation when a small volume is applied to an EM grid and most of the solvent wicked away before freezing. An alternative approach for preparing samples for cryo-ET is to subject tissues to high-pressure freezing, trim them partially in a cryo-microtome, followed by milling of thin lamellae in a dual beam cryo-focused ion beam/scanning electron microscope (FIB/SEM), transfer to a cryo-TEM and tomographic data acquisition [20,166]. This method has yet to be applied to photoreceptor sensory cilia, but it may be a promising approach for future studies.

A variation of electron microscopy that is potentially of great value is immuno-electron microscopy. Methods have not yet been developed for applying this technique in cryo-ET, but it has been used extensively in conjunction with conventional TEM, using either pre-embedding or post-embedding antibody labeling, with secondary labeling by gold particles or ferritin to provide a recognizable signal. This approach can provide invaluable information on localization at TEM resolution but struggles with several technical limitations. These include loss of immunoreactivity under the harsh fixation conditions used for TEM, and poor structure preservation and contrast under milder conditions of fixation and staining. In addition, each ultrathin section generally contains only a few visible antibody conjugates, and frequently also some conjugates not associated with the structures of interest, so distinguishing true signal from background and obtaining a three-dimensional picture of localization remain challenging. A promising approach for future studies may be combining genetically encoded electron-dense tags and tomographic or other 3D imaging methods.

Superresolution fluorescence offers the ability to localize specific macromolecules in two or three dimensions, and to image two or more targets at the same time, using antibody labeling or genetically-encoded tags. Three different modalities of superresolution microscopy have been applied to photoreceptor sensory cilia. Single-molecule localization microscopy (SMLM) which uses thousands of images of sparsely activated fluorophores in a dark background of fluorophores in a “dark” state to determine localization coordinates of single fluorophores with precision in the range from 5 nm to 50 nm. Following capture of each frame, the active fluorophores are inactivated by bleaching, and then a new round of photochemical or chemical reactivation allows capture of another sparse and randomly selected set of coordinates. A variation known as STORM (STOchastic Reconstruction Microscopy [72] has been used to localize a number of cilium-associated proteins and products of ciliopathy-associated genes in mouse rod cells [214,41,157]. A recent paper [105] has described application to zebrafish cone cells of Structured Illumination Microscopy [66], a technique in which multiple alternating patterns of illumination are used to shift high resolution information to lower resolution portions of the Fourier transform of images and computationally reassign it to improve resolution by about a factor of two. Application of SIM to rod cilia from mouse retina is described in a recently posted preprint [https://www.biorxiv.org/content/10.1101/2020.10.28.357806v1]. Another promising technique is STimulated Emission Depletion microscopy, STED [216,153], which uses a donut-shaped excited state depletion pulse tuned to the red edge of a fluorophore’s emission to obtain resolutions in the range of tens of nm.

An alternative approach to improve resolution of fluorescence-based localization is Expansion Microscopy, ExM [31,210], in which cytoplasm is essentially replaced with a hygroscopic cross-linked polymer network that expands all structures within it, in a more or less isotropic way, upon hydration. This approach has been successfully applied to the retina [163], although ciliary substructures were not visualized. There have been multiple reports of its successful application to both motile and primary cilia in other cell types [53,52,162,88,96,103,112,152,184,188,238].

As with immuno-EM, an ongoing challenge for immunofluorescence microscopy is the trade-off between conditions that maximize preservation of structure and those which maximize accessibility of antigenic epitopes to added antibodies. In single-molecule localization microscopy there is also a conflict between adequate labeling densities needed to ensure that desired image resolution is within the Nyquist sampling limit [101], and the need to avoid simultaneous emission from two fluorophores within the diffraction limit of one another. This problem may be alleviated by decreasing the probability of activation, e.g. using DNA-PAINT methodology [35,61] or photoactivation light microscopy (PALM [13]), albeit it at the expense of longer imaging times. All of the fluorescence methods mentioned above have been applied fairly extensively to primary and motile cilia of non-photoreceptor cells, as the unique structural features of cilia make them an ideal test bed for new methodologies. Much remains to be done to adapt these approaches optimally to retinal tissue.

Dimensions and Components of Photoreceptor Cilia and Associated Structures

Outer Segments and Connecting Cilia

Among vertebrate species, OS of rods and cones vary widely in size. A number of species have particularly large photoreceptors, including the mudpuppy, *Necturus*, whose rod OS measure approximately 12 μm in diameter by 30 μm in length, encompassing a volume of 3.4 pL [17]. Mice have rod OS measuring roughly 1–1.5 μm by 24 μm, with a nearly one hundred-fold lower volume of about 0.035 pL [183,110,23]. Human photoreceptors are comparably thin and can have OS as short as 3 μm (infant cones) to as long as 63 μm (adult foveal cones) [68,233]. Dimensions of the CC and associated structures have been determined in mice by cryo-ET [58]. The CC is roughly 1000 nm in length in mice; the diameter is about 300 nm, with some variations in diameter along its length. The inner diameter of the axoneme within the CC is 156 nm, and the diameters of the A microtubules and B microtubules of the doublets are 22 nm and 24 nm, respectively.

Basal body

The basal body (BB) lies at the base of all cilia and flagella and is composed of a pair of centrioles, which are ~302 nm long tubes formed around 9 bundled microtubule triplets arranged in a cylinder, and a compliment of associated pericentriolar structures. The centriole pair in the BB originates from the centrosome, where the older centriole, termed the mother centriole (MC), duplicates to form the daughter centriole (DC). The mother and daughter centrioles are generally positioned within about 500 nm of one another, with a fairly wide variation in this distance (±131 nm). The centrioles are generally depicted as having their long axes at right angles to one another, but in reality, there is a wide variation in this angle from cell to cell [58] (Fig. 6).

In the developing mouse retina during asynchronous rod photoreceptor ciliogenesis, nascent BB centrioles are typically observed in different positions as they migrate through the IS cytoplasm, between postnatal days P0 and P7, to eventually dock onto to the apical surface [170]. The MC of the nascent BB serves as the template for the formation of the axoneme

during ciliogenesis, and thus the nine MC microtubule triplets are continuous with the nine microtubule doublets in the axoneme of the CC in rod neurons. The DC remains in the IS cytoplasm near the MC [58]. In primary cilia the BB serves as a critical way station for ciliary cargo transport, and in rod cilia, the BB may be the way station for rhodopsin and other OS cargoes. It is therefore an active and essential region of the cilium, especially considering the high volume of trafficking that flows into the cilium from the IS.

Within and around the BB, numerous structures serve as potential docking sites for ciliary cargo proteins, including the pericentriolar material (PCM) that surrounds the BB centrioles, the centriolar satellites, and the distal and sub-distal appendages [33,124,140,225]. Although ciliary cargoes clearly accumulate at the BB with intraflagellar transport (IFT) proteins and motor proteins in rod CC, the organization of ciliary cargoes within the structures of the BB region of any primary cilium remains generally unexplored. See [134,167,147,79,7,198] for reviews of the roles of IFT proteins and motor proteins in trafficking to and from the cilium in photoreceptors and other cell types.

In recent years, the core structure of the centrioles of centrosomes and BBs has been extensively mapped using state-of-the-art cryo-ET imaging and expansion microscopy (ExM) [52,162,63].

The MC in the basal body of mouse rod photoreceptor cilia maintains the same appendage structures attached to the MC in the centrosome, namely the distal appendages (DAPs, also known as transition fibers) and the subdistal appendages (sDAPs). The DAPs and sDAPs are essential for centriole docking during ciliogenesis [203,195,9].

Distal appendages

The DAPs have been classically defined from conventional TEM micrographs as blades or pinwheel fins that attach to each of the 9 microtubule triplets of the distal end of the MC in a striking rotational symmetry [4]. These blades are found in photoreceptors to attach to the periciliary/ciliary membrane border in the BB. The DAP structure from a HeLa cell centrosome MC was recently modeled with fine detail using electron tomography (conventional TEM-based) [16]. The architecture of the blades was shown to be composed of finger-like fibers with a dense head region bound to two adjacent MT triplets. The following protein components of the DAPs were originally identified with proteomics and SIM imaging: CEP164, CEP89/CCDC123, CEP83/CCDC41, SCLT1, and FBF1 [195]. The 3D localization and organization of these DAP proteins was more recently thoroughly mapped with superresolution using STORM (stochastic optical reconstruction, a form of single molecule localization microscopy (SMLM)) [225] and correlative STORM/EM [16] as a blade pattern that closely matches the TEM structure. The STORM study also localized the core DAP protein FBF1 to the space between the blades that was termed the distal appendage matrix (DAM), and localized IFT88 specifically to this DAM region [225].

The association of the IFT proteins with the DAPs was also shown during ciliogenesis in developing mouse rods [170], and in adult mouse rods using immunoelectron microscopy, IFT52, IFT57, IFT88, and IFT140, which are all components of the IFT supramolecular transport particle, were densely localized in the region of the DAPs [169]. The potential

role of the DAPs in cell trafficking in adult rods is intriguing considering that the DAPs are located, structurally, at the interface of the BB and the CC, and may be an important checkpoint for ciliary trafficking. As such, the DAPs may contribute to the proposed barrier or gate for membrane cargo receptors at the base of the CC [171,227], or may serve as a docking surface for the coupling of ciliary cargoes to IFT proteins for transport into the cilium, as has been proposed in other models [74,211,229].

Using TEM and heavy metal stains, the DAPs are very evident in the BB of rod cilia and display a dense accumulation of stain (Fig. 6A). In cryo-ET tomograms of mouse rod cilia that are devoid of any TEM stains, the blade structures of DAPs are nearly invisible, indicating low electron density, and as such, the barrier between the BB cytoplasm and the CC is not clearly visualized. In the region of cryo-ET tomograms where DAPs are observed, there are fibers which are not observed with conventional TEM. They extend from the C-microtubules of the MC and associate with unassigned fibers of a different geometry that run parallel with the membrane and are observed tethered to cytoplasmic vesicles [58,157]. We recently immunolocalized the DAP protein CEP164 to the DAP region of the rod cilia (V. Potter et al., unpublished observations-see preprint: https://www.biorxiv.org/content/10.1101/2020.10.28.357806v1); however, the localization of the full complement of DAP proteins to the rod photoreceptor cilia may reveal a unique, photoreceptor-specific DAP geometry and composition.

Subdistal appendages

In mouse rods, the sDAPs are prominently observed at early postnatal ages using conventional TEM and heavy metal staining (P7 in Fig. 6B). The sDAPs are located proximal to the DAPs and do not appear to have 9-fold symmetry. They are composed of a varying number of triangular wings that link adjacent MC triplets [202]. The functions of the sDAPs have been studied only in centrosomes [15,33], and their roles in photoreceptor cilia are not known. The core protein components of the sDAPs were identified in centrosomes as ODF2, CEP128, centriolin, ninein, and CEP170, and these same proteins were recently mapped in cultured RPE cells using STORM to match the wing-shape structure [33]. Like the DAPs, the sDAPs in adult rod photoreceptor cilia are not visible in cryo-ET tomograms [58,157], but unlike the DAPs, there is no obvious role for the sDAPs in the dynamics of rod cilia post-ciliogenesis.

Pericentriolar material

Both centrioles of the BB are surrounded by an electron-dense proteinaceous coat or tube known as the pericentriolar material (PCM). The multiple protein components of the PCM and their localization have been identified, including CEP135, ninein, pericentrin, C-Nap-1/Cep250 and gamma tubulin, which forms a gamma (γ) tubulin ring complex (γTuRC) [143,234,81,124,219]. The γTuRC functions as a microtubule nucleation site for centrioles in the centrosome [121]. Although gamma tubulin is localized at the BB centrioles in isolated bovine rod photoreceptor cilia [126], cytoplasmic microtubules appear not to be linked to the BB/γTuRC in rods. One PCM protein that has been rigorously localized in the BB of photoreceptor cilia is pericentrin in a report by Mühlhans *et al.* [124]. With specific immunolocalization experiments, the large coiled-coil pericentrin protein was localized

surrounding the BB centrioles and more densely accumulated at the proximal (inward facing) triplet ends of the BB centrioles [124]. CG-Nap/AKAP9, another coiled-coil PCM protein, was also localized to the mouse rod BB in that study.

Centriolar satellites

The BB centrioles are surrounded by a matrix of electron dense mobile elements called the centriolar satellites that putatively serve as substrates and organizers for cilia-bound cargoes [124,140]. Unlike the PCM, the satellites are unorganized mobile granules that are membrane-less [40,140], and they were recently characterized as a membrane-less organelle (MLO), which are phase-transition cytoplasmic condensates caused by disordered domains within its constituent proteins [85]. The satellites are observed sporadically around the BB in TEM micrographs as electron-dense granules 70 – 100 μm in diameter [99]. They are difficult to identify in the dense IS cytoplasm of adult photoreceptor cilia; however, dense satellite granules were clearly observed with TEM in the BB region in mouse rods during the earliest stages of ciliogenesis [170]. Sedmak *et al.* [169] localized the IFT proteins IFT20, IFT52, IFT57, IFT88 and IFT140 to satellite structures in the BB of rod neurons during ciliogenesis by immunoelectron microscopy [170]. As the IFT proteins localize to the BB in adult rod cilia [169,157], the centriolar satellites are also potential substrates for maintaining a pool of IFT proteins and other trafficking machinery for eventual cilia cargo coupling and trafficking to the OS.

The satellite protein PCM1 (pericentriolar material 1) is the scaffold for other satellite proteins [70] and interacts with a large network of protein interactors as part of a comprehensive centriolar satellite interactome that has been characterized by a number of groups using proximity mapping [55,37,140]. PCM1 was localized to the BB region in adult mouse photoreceptors [124,45]. In another study, RP2, the protein product of a retinitis pigmentosa-associated gene, which serves as a GTPase activating protein for Arl3, an essential small GTPase regulator of CC trafficking, was localized by immunoelectron microscopy to the BB and tentatively to the centriolar satellites of rods [44].

Other notable interactions between centriolar satellite proteins and key photoreceptor trafficking regulators have been reported. The Bbs (Bardet-Biedl syndrome ciliopathy) protein subunits form a BBSome complex [132,131,224,34,109,174], whose function is required to avoid accumulation of inappropriate proteins in the CC and outer segment and to prevent retinal degeneration. BBS4 colocalizes and interacts with PCM1. BBS4 is essential for the normal localization of the BBSome to the BB of primary cilia [93,132,236,89]. BBS4 also interacts with the satellite proteins AZI1/Cep131 [30]. Cep290 is a large cilium-associated protein whose encoding gene is associated with multiple ciliopathies, and is the most common cause of the childhood blinding disease Leber Congenital Amaurosis [200]. CEP290 was reported to co-localize and interact with PCM1 in the BB of primary cilia [92], via another cilium/centrosome-associated protein, Cep72 [186]. Cep290 also interacts with the centriolar satellite proteins SSX2IP and CP110 in the BB [94,201]. In mouse rod photoreceptors, Cep290 and BBSome protein subunits have been localized to the BB [1,176,41,157] (V. Potter et al., unpublished observations-see preprint: https://www.biorxiv.org/content/10.1101/2020.10.28.357806v1). As with the BB pool of IFT

proteins, the centriolar satellites are candidates for maintaining and organizing the pool of ciliary machinery at the BB in rods.

Periciliary membrane

The IS plasma membrane that is adjacent to the CC is known as the periciliary membrane in mouse rods or the periciliary ridge in Xenopus rods [114]. In each case, they serve to form the ciliary pocket, an in-folding of the membrane at the base of the cilium, and they contain a complement of proteins distinct from those elsewhere in the IS membrane.

Rho and Rho-containing IS transport vesicles were shown to localize with the periciliary membrane in mouse rods and the periciliary ridge in *Xenopus* rods, which may serve as a docking site for these vesicles [145,25,114,150]. In mice, the periciliary-CC membrane interface is maintained by the periciliary membrane complex (PMC). The PMC contains Usher syndrome-related proteins, including myosin VIIa, VLGR1, and whirlin, and physically links the CC and periciliary membranes. It is distinctly localized to one side of the CC in mouse rods [223,157,111]. Usher proteins are also localized in the periciliary ridge (Maerker et al., 2008). The potential coordination of Rho cargo docking between the PMC and the BB, and the impact of this docking on Rho trafficking through the CC, have not been characterized.

Because of the dense networks of fibers and filaments of varying diameters, it is somewhat difficult to visualize the network of microtubules linked to the periciliary matrix. Cytoplasmic microtubules have been observed in the apical IS of human rods with TEM [111], and cytoplasmic dynein motors were shown to move rhodopsin containing vesicles along microtubules *in vitro* [191].

Ciliary rootlet

The ciliary rootlet is a prominent cytoskeletal element throughout the biosynthetic regions of mammalian rod photoreceptor neurons that is directly linked at its distal end to the BB [175,182,36,58,219]. The thick, filamentous rootlet extends proximally from the BB through the IS cytoplasm, into the outer nuclear layer (ONL) surrounding the soma and terminates at the synapse in the outer plexiform layer (OPL) [36,175,182]. In electron micrographs the rootlet is characteristically striated (Fig. 6C), which is caused by rootletin, the core cytoskeletal protein of the rootlet, which has an elongated coiled-coil tail domain that homopolymerizes into parallel, overlapping bundles that form the striated rootlet filament [222].

Although the 220-kD rootletin protein was first identified in mouse rod photoreceptors, the rootlet is a structural component of the motile cilia and flagella of various species and cell types. Unlike in mammalian photoreceptors, those rootlets serve to stabilize the beating or waving action the ciliary or flagellar axonemes [118]. Flagellar rootlets are particularly divergent from photoreceptor rootlets as, in response to Ca^{2+} influx they under contractions mediated by centrins, which are small Ca^{2+} binding proteins [199,164]. The photoreceptors of poikilotherms, including in the retinas of *Xenopus* frog species, do not have obvious ciliary rootlets. In mammals, loss of rootlets affects stability, viability and visual pigment transport at older ages in both rods and cones [58,220].

The role of the rootlet in normal rod photoreceptor function remains unclear. Retinas from knockout mice of *Crocc* (ciliary rootlet coiled-coil, the gene encoding rootletin) were morphologically unaffected, including normally localized BB centrioles, even though the rod photoreceptors were missing rootlets, as observed by TEM [220]. Only after 12 months do these mice display signs of photoreceptor dystrophy. After the mechanical stress of being isolated from the retina, however, rod outer segment cilia from rootletin knockout mice were fragile [220], and when reconstructed with cryo-ET, were seen to have a broken and dysmorphic ciliary axoneme [58]. As such, the rootlet for rod cilia is not necessary for normal photoreceptor function, but the fragility that rises from the lack of the rootlet does seem to promote photoreceptor cell death. It may be one of many supportive, but not essential, features of photoreceptor cilia that confer robustness of function in the presence of environmental or genetic stress.

The rootlet is linked directly to the BB centrioles in rods through an interaction between rootletin and C-Nap1/Cep250, a rootletin homolog [219] and a PCM protein that was recently associated with nonsyndromic retinitis pigmentosa [73]. C-Nap-1 fibers are localized at the proximal ends of the BB centrioles [219], although, this localization has not been established in photoreceptors. In cryo-ET tomograms of isolated mouse rod IS/OS fragments, a nest of fibers is evident in the space between the BB centrioles, and it is still present in rootletin knockout rods [58]. These fibers potentially correspond to C-Nap, which may function as a scaffold between the centrioles, even in the absence of a connected rootlet.

The large size of the rootlet in mammalian rods, and the large volume of space it occupies within the rod IS suggest that the rootlet may serve as a convenient organizer or trafficking route for cytoplasmic proteins and organelles. Such a role, if it exists, would have to be redundant with other mechanisms, as only defects in long-term stability, and no acute trafficking defects, are apparent in rootletin knockout mice. As it is directly linked to the BB, the rootlet is structurally placed to serve as a potential highway through the IS to the BB for ciliary trafficking cargo. In many conventional TEM images of the rod IS, the rootlet is associated with IS mitochondria or cytoplasmic membranes described as “saccules” throughout the literature. These vesicular membrane saccules were postulated to be ER membranes that apparently contact the rootlet at various points throughout the rod IS in an unorganized manner [182,217,222,220]. In one report, the saccules were observed to be contiguous with rough ER. In cryo-ET tomograms of the rod IS, proteinaceous densities and occasional lateral filaments were found along the rootlet [58]. F-actin was not localized at the ciliary rootlet in monkey rod IS with immunoelectron microscopy [27], leaving the composition of these filaments undetermined.

The globular head domain of rootletin displays promiscuous binding, including non-specific binding to antibodies used as immunolabeling reagents [114]. This sticky surface may be what anchors and maintains the contact between the rootlet and IS organelles. Rootletin, through its globular head domain, was shown to interact with kinesin light-chain (KLC) 1–3 protein subunits of the kinesin-I and -II motor proteins [222,221]. In a curious finding, peripherin/rds, an integral OS disc rim protein, was localized via immunoelectron microscopy to vesicles bound to the rootlet, but only in rods from mice with experimentally detached retinas [47]. Non-vesicular particles were also visualized on the surface of the

rootlet, and the size distribution of these varies substantially between dark-adapted and light-adapted conditions, suggesting a role in ciliary dynamics [58]. Thus far, these are the only characterized interactions that link any aspect of cellular trafficking in the rod IS to rootletin.

Despite these observations, the relative functional normality of photoreceptor cilia in intact retina of rootletin knockout mice suggests that the rootlet is not necessary for the biosynthesis and cellular trafficking of material to the OS cilia. The robust nature of the vectorial transport of materials in the rod IS may enable rod cells to process and transport cargo along alternative redundant pathways. For example, peripherin/rds itself was shown to utilize a non-conventional secretory pathway that bypasses the convention vesicular route through the Golgi [197], potentially through a late endosome pathway [142]. Therefore, the rootlet may normally serve as a substrate or organizer for trafficking in rod photoreceptors, and in rootletin knockout rods those processes must use an alternative or redundant substrate, such as cytoplasmic microtubules.

Structures and complexes within the connecting cilium.

The arrangement of microtubules varies along the length of sensory cilia, as does the complement of accessory structures and proteins associated with the outsides and insides of the microtubules. These also vary among cell types and species [82]. Throughout most of the BB, each tubule is composed of triplet microtubules, A-B-C, whereas at the distal ends of both centrioles there are partial triplets, *i.e.,* A-B doublets with attached incomplete C-tubules [62,63,106], which transition to doublets in both centrioles of photoreceptors. Each tubule possesses 13 or 10 microtubule protofilaments, respectively. The A-tubule is characterized by a ring structure, and is the tubule that continues on in the singlet region, and the B-tubule is characterized by a c-shape which joins the A-tubule at two places, the inner and outer junction [136,107]. The inner junction (IJ) also contains an 11^{th} non-tubulin protofilament, which is thought to be made by the proteins Flagella Associated protein 20 (FAP20), Parkin Coregulated Gene Protein (PACRG), and Tektin [76,218]. Beyond the zone where the transition from incomplete triplets to doublets occurs, at the distal end of the MC in the region of the distal appendages described above, the axoneme begins as a bundle of 9 microtubule doublets (Fig. 1). As these progress distally, they undergo loss of the B-tubule and become singlets [80]. In the proximal region, doublets and 9-fold symmetry persist for various distances in different cell types, but toward the more distal regions, the doublets transition to singlets, the 9-fold symmetry is lost, and the number of microtubules declines, often to a single one at the tip [57,80,189].

The nomenclature of ciliary subdomains in the literature is somewhat diverse and confusing. The basal body, as discussed above, can be clearly defined as a pair of centrioles, at a roughly orthogonal angle, built predominantly around a core of 9 microtubule triplets, about 300 nm long. In contrast, the “transition zone” (TZ), if defined as the region of transition from triplet to doublet microtubules is, in both motile and non-motile cilia, no more than 100 or 200 nm in extent; this transition also occurs in the DC at the distal end facing away from the MC in rods [214], and to triplets with “partial” C microtubules in some other ciliated cells [62]. In contrast, if the “transition zone” is defined in terms of specific

macromolecular complexes or structural elements visualized by electron microscopy, such as the “NPHP complexes,” the “MKS complex” (TCTN1, TCTN2, TMEM231, TMEM67, MKS1, MKS6, B9D1, B9D2, and AHI1), the “ciliary necklace” or “Y-shaped links” (see descriptions of these below), its length varies dramatically among species and cell types. Indeed, even the consistent markers of the TZ region segregate into distinct subregions when visualized at nanoscale resolution [226,157,41]. In a STED imaging study of primary cilia in cultured RPE-1 cells, CEP290 was observed restricted to a region of about 50 nm beyond the distal edge of CEP164 (distal appendage), with additional TZ markers, RPGRIP1L, MKS1, TMEM67 and TCTN2 located roughly 100 nm more distally [226]. In contrast, in a study of motile cilia in *Paramecium*, CEP290 was localized to a distal sub-compartment of the TZ, adjacent to RPGRIP1L and TMEM107, but more distal than NPHP4 and TMEM216 [60]. It has been suggested, based on distribution of key marker proteins, that a distinction be made between the proximal TZ, marked by “Group I” NPHP proteins, NPHP1, NPHP4, NPHP8/RPGRIPL1, NPHP5/IQCB1, and NPHP6/CEP290, and a more distal “Inversin/Inv” compartment, marked by NPHP2/INV, NPHP3 and PPHP9/Nek8 [173]. In rods, some proteins commonly associated with the proximal TZ of primary and motile cilia, such as CEP290, AHI1, NPHP1, and NPHP4 are distributed throughout the length of the connecting cilium [41] (see also https://www.biorxiv.org/content/10.1101/2020.10.28.357806v1). A similar longitudinal distribution is observed for photoreceptor-specific ciliary proteins SPATA7, RPGR and RPGRIP, and all of these become confined to the proximal TZ in the absence of SPATA7 [41].

Ciliary Necklace and Y-links

Freeze-fracture scanning electron tomographs of the ciliary membrane in 1972 revealed a unique structure surrounding the membrane at the base of the cilium, which the authors referred to as a ciliary necklace, due to its “beads on a string” appearance [59]. The necklace was described as consisting of three scalloped rows of protrusions, and tentatively associated with the Y-links [59]. Through further examination of multiple cilia types, the authors surmised that this necklace corresponded to “champagne glass” structures connecting the doublet-microtubules to the membrane, seen in ciliary cross-sections. These filamentous structures are now referred to as Y-shaped links, named for their “Y” appearance in electron micrographs of cross-sections stained with heavy metals [59,156]. However, the match between the angular distributions and apparent symmetries (or lack thereof) of the Y-links and necklace protrusions is not obvious, and cross-sections showing Y-links do not, in general, show obvious protrusions from the ciliary membrane in register with them. Their structural relationship has not undergone intense scrutinization with current superresolution techniques, and their distributions along the lengths of cilia are variable.

Both the necklace and Y-shaped links are generally conserved structural elements of eukaryotic flagella and cilia, although their distributions along the length of the cilia differ among cell types and organisms. Each link radiates from a microtubule doublet pair at the outer junction of the A and B tubules and bifurcates as it extends toward the membrane [156,71,59]. In gill cilia, the portion of the Y-link near the axoneme measures 15 nm, while the diameter of the bifurcation is 52 nm [59]. In eukaryotic flagella, longitudinal electron micrographs depict wedges in the TZ between the microtubule doublets and the

membrane, and these wedges do not occupy the entirety of the flagellar TZ. It is unclear, however, if the wedges in longitudinal views are the same Y-shaped links observed in cross sections, especially considering that the wedges observed in flagella are absent in longitudinal views of primary cilia [156]. Recent serial electron tomography of fixed epithelial cilia revealed irregular clumps of material connecting doublets to the membrane in the most proximal region of ~100 nm at the ciliary base [189]. Additional microtubule-to-membrane connections were observed in more distal regions, but not in a regular pattern. In photoreceptors, the Y-shaped links are observed along the full length of the connecting cilia (https://www.biorxiv.org/content/10.1101/2020.10.28.357806v1). The “Yshape” is observed in cross sections of the CC, however detergent extraction of membrane lipids reveals a more “tree”-like structure [71], agreeing with recent electron tomography studies of cilia and suggesting that the true structure in three dimensions may not be “Y-like” [58,189,215,157]. This idea also agrees with the original “champagne glass” description [59], in which the “Y” is the circular part of the glass and therefore has a round structure.

To date, the composition of the Y-shaped links and the necklace is unknown, though it has been hypothesized that CEP290 may form/interact with the Y-shaped links based on genetic and immunoimaging studies of *Chlamydomonas* flagella [38]. The immuno-EM data in that report, acquired using both C-terminal and N-terminal tags, actually suggest its localization to a region between two Y-shaped links, in closer proximity to one than the other. Since many TZ proteins appear to be part of stable structures, it is possible that any and/or many of them are involved in Y-shaped link and necklace formation or positioning. Further molecular imaging experiments, and the use of TZ mutant animals in which the Y-shaped links do not form will be needed to tease out the protein make-up of these structures.

The exact functions of the Y-shaped links and the necklace are also yet to be determined. It was originally hypothesized that the role of the Y-shaped links and ciliary necklace is to act as a switch for ciliary beating, regulated by Ca^{2+} signaling [59]. The Y-shaped links have been proposed to provide stability to the CC, as well as to create a barrier between the inner and OS, and aid in membrane protein trafficking [125]. These ideas, as well as the idea that nucleoporins such as NUP62 “filter” cytoplasmic proteins from diffusing into the cilium [14,90,192–194], have not been rigorously tested in rods or cones.

Although the photoreceptor cilium is highly modified in function, the basic structure of the CC is consistent with the proximal portion (including the TZ) of immotile primary cilia seen in other tissues, containing a 9+0 (i.e., a ring of 9 microtubule doublets lacking the central pair of microtubules found in motile cilia) microtubule morphology. Distal to the CC, at the base of the outer segment, the arrangement of nine microtubule doublets takes a form closer to triangular in cross section than to the 9-fold symmetric circle seen in the CC, and more distally, the microtubule arrangement undergoes a switch from doublet microtubules to singlet microtubules approximately one-third of the way up the axoneme, with singlets extending far into the OS length ([17,185,95,80,214]). This long singlet extension is rare and only observed in a few other cilia types, such as frog olfactory cilia and *C. elegans* sensory cilia [177,155]. Though this singlet extends deep into the OS length, it is unknown if it extends all the way to the tip of the OS.

At the base of the outer segment/distal end of the CC, there is an out-folding of the ciliary membrane to form nascent discs (Fig. 1), whose lumenal compartments are continuous with the extracellular space [204,19], unlike the more distal closed discs found in rod (but not cone) OS. In this region there are clusters of filamentous actin [58,26,28,29] which may be involved in this out-folding/evagination process, in conjunction with regulation by the Arp2/3 branching proteins [181,180]. RPGR, or a retina-specific splice variant of RPGR may be involved in this actin-dependent process [91,127,128,237,117].

Turnover and trafficking

The microtubules of the photoreceptor cilium are attached to the continually renewing membranous stacked discs where phototransduction occurs [230]. Rods and cones impose major demands for regulation of developmental processes such as OS formation as well as maintenance of function by selective trafficking of OS proteins to their site of action. This need is exacerbated by the fact that the outer segment goes through a daily process of shedding and renewal, so that every 10 days or so (in mammals) the entire OS is renewed as described above [230]. A similar flux occurs in species with longer OS, albeit with a greater time lack between synthesis and shedding of discs.

An estimate of the numbers of macromolecules and membrane components that must pass through this compartment can be obtained by considering the continual turnover of the disc membranes. Disc turnover is approximately 10% of a mouse rod per day and similar rates are observed in other mammals [230,231,102]; the major components are rhodopsin and phospholipid. The content of rhodopsin is 7×10^7 molecules (Lyubarsky et al, 2004; Driesen et al, 2000), so 7×10^6 molecules of rhodopsin must be transported every day, or approximately 800 per second. The phospholipid content is 60 per rhodopsin [113], so more than 48,000 phospholipid molecules must be transported per second. Turnover of guanine nucleotides [3] in rabbit rods as measured by mass spectrometry, is about 28.3 μM s^{-1} in the dark. If we assume a volume of about 19 fL, this corresponds to 316,000 molecules of GTP and ATP transported per second and an equal flux of 5’-GMP and 5’-AMP flowing in the opposite direction. According to a model that fits electrophysiological data well [65], cGMP turnover ranges from 16.7 μM s^{-1} in the dark to a maximum of 150 μM s^{-1} at saturating light levels in mice, in reasonable agreement with the MS data. A similar flux of NADPH or other reducing molecules must occur in the light to keep all-*trans* retinal in the mostly reduced state [2].

Cilia formation, *i.e.* ciliogenesis, in photoreceptor cells must be efficiently regulated to allow for creation of a functional, organized outer segment (OS) with stacked membrane discs that are packed with the phototransduction and structural proteins necessary for sight. The demand for efficient protein trafficking in the mature OS is a result of the anatomy of the photoreceptor cell which has distinct compartments, i.e. the IS where OS proteins are synthesized and the OS where those proteins must function to capture light [130]. Correspondingly, human disease may result from inefficiency in the process of protein trafficking in photoreceptor cells. Notably, mutations that disrupt the transport of phosphodiesterase 6 (PDE6), rhodopsin, or other phototransduction proteins are a major

cause of the blinding disease, retinitis pigmentosa (RP) [208,75]. RP alone is responsible for vision loss in 1 in 4,000 people worldwide [190].

Several reviews in the last few years provide in-depth discussion of trafficking in photoreceptors [50,209,148,79,77,11]. Selective transport to the CC and OS seems to involve a combination of active transport from the IS, involving microtubule-associated motor proteins such as kinesins and dyneins, passive diffusion with filtering mechanisms for both soluble and membrane proteins, and active retrograde transport. The BBSome complex, formed by proteins encoded by the Bardet-Biedl syndrome (BBS) genes appears to be critical for removal of inappropriate proteins from the CC and OS [228,134,131,54,132]. The proteins of the A and B intraflagellar transport complexes (IFTA and IFTB) ferry cargos in both directions along the photoreceptor axoneme, in conjunction with motor proteins [87,206,134,105,98,146,79] and are essential for the proper development and maintenance of the photoreceptors and their cilia. In addition to their accumulation at sites at or near the basal body complex described above, both IFT proteins and BBS proteins are found in clusters along the CC, presumably caught in the act of cargo transport [157]. Transport of lipidated proteins requires chaperoning by a prenyl binding protein also known and PDEδ, or UNC119, which binds fatty acyl chains [50,67,46,8], in a process regulated by the small GTPases Arl2 and Arl3.

Ciliogenesis

Ciliogenesis is an asynchronous process [178,170,64]. There are two different ciliogenesis pathways – intracellular and extracellular. In intracellular ciliogenesis, the cilium forms within a vesicle in the cytoplasm prior to extracellular exposure, whereas in extracellular ciliogenesis, the basal body docks at the plasma membrane before extending the axoneme extracellularly. Cultured cell ciliogenesis may occur intracellularly or extracellularly, depending on the position of the centrosome in relation to the plasma membrane. Cell types with centrioles closer to the nucleus undergo intracellular ciliogenesis, while centrioles closer to the cell surface undergo extracellular ciliogenesis. This section will primarily focus on intracellular ciliogenesis, which is the pathway employed by photoreceptors. Intracellular ciliogenesis can be divided into stages, discussed below.

Primary ciliary vesicle

The first stage occurs within the cytoplasm and involves the primary ciliary vesicle [178]. The primary ciliary vesicle appears at the distal end of the MC centriole [178,149], and later flattens to become the ciliary sheath surrounding the ciliary bud. The subdistal and distal appendages then localize to the MC centriole and aid in stabilizing and anchoring the MC centriole to the primary ciliary vesicle for ciliogenesis (see Distal Appendages and Subdistal Appendages sections above for list of involved proteins) [178,179]. The distal appendages anchor the MC centriole to the vesicle for docking, and are sometimes referred to as “transition fibers” (Figs. 6, 7) [149].

Ciliary Shaft

In the second stage, the ciliary bud extends to become the ciliary shaft (Fig. 7). The extension of the ciliary shaft requires the intraflagellar transport (IFT) system, which is

a bidirectional microtubule-based motility process mediated by IFT particles and motor proteins. The current model is that kinesin-2 motor proteins and the IFT B complex (containing a subset of IFT proteins) participate in anterograde transport, while dynein 2 motor proteins and IFT A complex (with an overlapping but different subset) are involved in retrograde transport [170,149,161].

These particles move along the axoneme delivering tubulin subunits and other axonemal components from the cell body, where they are synthesized, to the ciliary tip for axonemal extension. They also retrieve axonemal components and recycle IFT B complex from the ciliary tip back to the ciliary base [149,161]. Additionally, the kinesin 2 motor stabilizes the growing plus ends of microtubules to facilitate tubulin incorporation [83]. The IFT particles and motors are necessary for axonemal assembly and maintenance. In their absence, the axoneme either does not form or regresses [84]. As the ciliary shaft lengthens, secondary Golgi-derived vesicles fuse with the ciliary sheath membrane to lengthen it [178,64].

Plasma membrane fusion

In the third stage, the sheath membrane interacts and fuses with the plasma membrane, exposing the cilium to the external environment [178]. This fusion leads to the formation of a subdomain of the plasma membrane called the ciliary pocket (Fig. 7C) [120,56], which later becomes the periciliary ridge/membrane. Within these pockets, clathrin coated pit proteins localize, and there is active endocytosis [120]. The ciliary pocket may also serve as a site for the release of Golgi-derived secretory vesicles. IFT20 and IFT52 both localize to the ciliary pockets and associate with Golgi-derived vesicles [169].

Disc morphogenesis

The last stage is unique to photoreceptors and involves outer segment formation and maturation (Fig. 7D). As the cilium extends extracellularly, the proximal cilium gives rise to the CC and the distal cilium gives rise to the outer segment. Disc morphogenesis is mediated by evagination of the ciliary plasma membrane at the base of the OS [19,42]. Initially the discs are open to the extracellular space and contact the periciliary ridge, an IS structural complex that partially surrounds the CC [150] via PCDH21, a photoreceptor-specific protocadherin [19,154]. However, in rod photoreceptors, as the open discs move distally, the leading edge of an evaginated membrane fuses with an adjacent evagination to form a closed disc. While the disc is open, peripherin, an OS disc protein known for organizing the disc rims in complex with Rom-1, is only present at the rim near the axoneme, but once disc closure occurs peripherin is redistributed throughout the rim [19,42,122,5,119]. Coupled with disc closure is the loss of the IS connection mediated through PCDH21 [19].

Outstanding questions and challenges

Advances in imaging techniques, combined with both human genetics and a large number of animal models, have led to tremendous advances in our understanding of photoreceptor sensory cilia. Despite this progress, many of the most fundamental questions about their structures and dynamics remain unanswered. For the most part, the exact molecular composition of the substructures of cilium-associated structures remains unknown, much less the precise locations of specific molecules within them. For many ciliopathies in human

patients and animal models, the primary defects leading ultimately to loss of ciliary function and cell death, as opposed to defects such as impaired trafficking that may be secondary to the initial defects, remain poorly understood. Fortunately, these problems have attracted many talented and dedicated investigators, and the tools available are increasingly powerful. Hopefully, in the near future, application of these tools to establish genetically-encoded nanoscale tags and image them at the molecular scale will lead to a series of major breakthroughs in this area. An ongoing challenge is to monitor dynamics and trafficking in real time because the currently available methods generally depend on optical methods and photoreceptors are extremely sensitive to light. Some advances in the use of multiphoton excitation via infrared lasers have been reported [133,22,21,77,108,196,78], and this seems to be a promising direction for future studies of photoreceptor ciliary dynamics.

Acknowledgements

The authors acknowledge support from the National Eye Institute of the U.S. National Institutes of Health (R01-EY026545, R01EY031949, F32 EY027171, F31-EY028025, T32-EY007102), the Knights Templar Eye Foundation, and the Robert A. Welch Foundation (Q0035).

Funding:

Provided by the National Eye Institute of the U.S. National Institutes of Health (R01-EY026545, R01-EY031949, F32-EY027171, F31-EY028025, T32-EY007102), the Knights Templar Eye Foundation, and the Robert A. Welch Foundation (Q0035).

Availability of data and material:

Not applicable

Abbreviations

IS	Inner Segment
OS	Outer Segment
ONL	outer nuclear layer
OPL	outer plexiform layer
CC	connecting cilium
BB	basal body
TZ	transition zone
PCM	pericentriolar material
DC	daughter centriole
MC	mother centriole
DAM	distal appendage material
CP	ciliary pocket

DAP	distal appendage
sDAP	subdistal appendage
PCV	primary ciliary vesicle
TF	transition fibers
IFT	intraflegellar transport
MT	microtubule

References

1. Abd-El-Barr MM, Sykoudis K, Andrabi S, Eichers ER, Pennesi ME, Tan PL, Wilson JH, Katsanis N, Lupski JR, Wu SM (2007) Impaired photoreceptor protein transport and synaptic transmission in a mouse model of Bardet-Biedl syndrome. Vision Res 47:3394–3407. doi:S0042-6989(07)00399-9 [pii] 10.1016/j.visres.2007.09.016 [PubMed: 18022666]
2. Lt Adler, Chen C, Koutalos Y (2014) Mitochondria contribute to NADPH generation in mouse rod photoreceptors. J Biol Chem 289:1519–1528. doi:10.1074/jbc.M113.511295 [PubMed: 24297174]
3. Ames A 3rd, Walseth TF, Heyman RA, Barad M, Graeff RM, Goldberg ND (1986) Light-induced increases in cGMP metabolic flux correspond with electrical responses of photoreceptors. J Biol Chem 261:13034–13042 [PubMed: 2875993]
4. Anderson RG (1972) The three-dimensional structure of the basal body from the rhesus monkey oviduct. J Cell Biol 54:246–265 [PubMed: 5064817]
5. Arikawa K, Molday LL, Molday RS, Williams DS (1992) Localization of peripherin/rds in the disk membranes of cone and rod photoreceptors: relationship to disk membrane morphogenesis and retinal degeneration. J Cell Biol 116:659–667. [PubMed: 1730772]
6. Asano S, Engel BD, Baumeister W (2016) In Situ Cryo-Electron Tomography: A Post-Reductionist Approach to Structural Biology. J Mol Biol 428:332–343. doi:10.1016/j.jmb.2015.09.030 [PubMed: 26456135]
7. Avasthi P, Watt CB, Williams DS, Le YZ, Li S, Chen CK, Marc RE, Frederick JM, Baehr W (2009) Trafficking of membrane proteins to cone but not rod outer segments is dependent on heterotrimeric kinesin-II. J Neurosci 29:14287–14298. doi:10.1523/JNEUROSCI.3976-09.2009 29/45/14287 [pii] [PubMed: 19906976]
8. Baehr W (2014) Membrane protein transport in photoreceptors: the function of PDEdelta: the Proctor lecture. Invest Ophthalmol Vis Sci 55:8653–8666. doi:10.1167/iovs.14-16066 [PubMed: 25550383]
9. Baehr W, Hanke-Gogokhia C, Sharif A, Reed M, Dahl T, Frederick JM, Ying G (2019) Insights into photoreceptor ciliogenesis revealed by animal models. Prog Retin Eye Res 71:26–56. doi:10.1016/j.preteyeres.2018.12.004 [PubMed: 30590118]
10. Barber CF, Heuser T, Carbajal-Gonzalez BI, Botchkarev VV Jr., Nicastro D (2012) Three-dimensional structure of the radial spokes reveals heterogeneity and interactions with dyneins in Chlamydomonas flagella. Mol Biol Cell 23:111–120. doi:10.1091/mbc.E11-08-0692 mbc.E11-08-0692 [pii] [PubMed: 22072792]
11. Barnes CL, Malhotra H, Calvert PD (2021) Compartmentalization of Photoreceptor Sensory Cilia. Front Cell Dev Biol 9:636737. doi:10.3389/fcell.2021.636737 [PubMed: 33614665]
12. Bell JM, Chen M, Durmaz T, Fluty AC, Ludtke SJ (2018) New software tools in EMAN2 inspired by EMDatabank map challenge. J Struct Biol 204:283–290. doi:10.1016/j.jsb.2018.09.002 [PubMed: 30189321]
13. Betzig E, Patterson GH, Sougrat R, Lindwasser OW, Olenych S, Bonifacino JS, Davidson MW, Lippincott-Schwartz J, Hess HF (2006) Imaging intracellular fluorescent proteins at nanometer resolution. Science 313:1642–1645. doi:10.1126/science.1127344 [PubMed: 16902090]

14. Blasius TL, Takao D, Verhey KJ (2019) NPHP proteins are binding partners of nucleoporins at the base of the primary cilium. PLoS One 14:e0222924. doi:10.1371/journal.pone.0222924 [PubMed: 31553752]
15. Bornens M (2002) Centrosome composition and microtubule anchoring mechanisms. Curr Opin Cell Biol 14:25–34. doi:10.1016/s0955-0674(01)00290-3 [PubMed: 11792541]
16. Bowler M, Kong D, Sun S, Nanjundappa R, Evans L, Farmer V, Holland A, Mahjoub MR, Sui H, Loncarek J (2019) High-resolution characterization of centriole distal appendage morphology and dynamics by correlative STORM and electron microscopy. Nat Commun 10:993. doi:10.1038/s41467-018-08216-4 [PubMed: 30824690]
17. Brown PK, Gibbons IR, Wald G (1963) The Visual Cells and Visual Pigment of the Mudpuppy, Necturus. J Cell Biol 19:79–106. doi:10.1083/jcb.19.1.79 [PubMed: 14069804]
18. Bui KH, Ishikawa T (2013) 3D structural analysis of flagella/cilia by cryo-electron tomography. Methods Enzymol 524:305–323. doi:10.1016/B978-0-12-397945-2.00017-2 B978-0-12-397945-2.00017-2 [pii] [PubMed: 23498747]
19. Burgoyne T, Meschede IP, Burden JJ, Bailly M, Seabra MC, Futter CE (2015) Rod disc renewal occurs by evagination of the ciliary plasma membrane that makes cadherin-based contacts with the inner segment. Proc Natl Acad Sci U S A 112:15922–15927. doi:10.1073/pnas.1509285113 [PubMed: 26668363]
20. Bykov YS, Schaffer M, Dodonova SO, Albert S, Plitzko JM, Baumeister W, Engel BD, Briggs JA (2017) The structure of the COPI coat determined within the cell. Elife 6. doi:10.7554/eLife.32493
21. Calvert PD, Peet JA, Bragin A, Schiesser WE, Pugh EN Jr. (2007) Fluorescence relaxation in 3D from diffraction-limited sources of PAGFP or sinks of EGFP created by multiphoton photoconversion. J Microsc 225:49–71. doi:10.1111/j.1365-2818.2007.01715.x [PubMed: 17286695]
22. Calvert PD, Schiesser WE, Pugh EN Jr. (2010) Diffusion of a soluble protein, photoactivatable GFP, through a sensory cilium. J Gen Physiol 135:173–196. doi:10.1085/jgp.200910322 jgp.200910322 [pii] [PubMed: 20176852]
23. Carter-Dawson LD, LaVail MM (1979) Rods and cones in the mouse retina. I. Structural analysis using light and electron microscopy. J Comp Neurol 188:245–262. doi:10.1002/cne.901880204 [PubMed: 500858]
24. Castano-Diez D, Zanetti G (2019) In situ structure determination by subtomogram averaging. Curr Opin Struct Biol 58:68–75. doi:10.1016/j.sbi.2019.05.011 [PubMed: 31233977]
25. Chadha A, Volland S, Baliaouri NV, Tran EM, Williams DS (2019) The route of the visual receptor rhodopsin along the cilium. J Cell Sci 132. doi:10.1242/jcs.229526
26. Chaitin MH (1991) Actin filaments in the photoreceptor cilium of the rds mutant mouse. Exp Eye Res 53:107–113. doi:0014-4835(91)90152-5 [pii] [PubMed: 1879494]
27. Chaitin MH, Bok D (1986) Immunoferritin localization of actin in retinal photoreceptors. Invest Ophthalmol Vis Sci 27:1764–1767 [PubMed: 3793408]
28. Chaitin MH, Burnside B (1989) Actin filament polarity at the site of rod outer segment disk morphogenesis. Invest Ophthalmol Vis Sci 30:2461–2469 [PubMed: 2592159]
29. Chaitin MH, Schneider BG, Hall MO, Papermaster DS (1984) Actin in the photoreceptor connecting cilium: immunocytochemical localization to the site of outer segment disk formation. J Cell Biol 99:239–247 [PubMed: 6610682]
30. Chamling X, Seo S, Searby CC, Kim G, Slusarski DC, Sheffield VC (2014) The centriolar satellite protein AZI1 interacts with BBS4 and regulates ciliary trafficking of the BBSome. PLoS Genet 10:e1004083. doi:10.1371/journal.pgen.1004083 [PubMed: 24550735]
31. Chen F, Tillberg PW, Boyden ES (2015) Optical imaging. Expansion microscopy. Science 347:543–548. doi:10.1126/science.1260088 [PubMed: 25592419]
32. Chen M, Bell JM, Shi X, Sun SY, Wang Z, Ludtke SJ (2019) A complete data processing workflow for cryo-ET and subtomogram averaging. Nat Methods 16:1161–1168. doi:10.1038/s41592-019-0591-8 [PubMed: 31611690]
33. Chong WM, Wang WJ, Lo CH, Chiu TY, Chang TJ, Liu YP, Tanos B, Mazo G, Tsou MB, Jane WN, Yang TT, Liao JC (2020) Super-resolution microscopy reveals coupling between mammalian centriole subdistal appendages and distal appendages. Elife 9. doi:10.7554/eLife.53580

34. Chou HT, Apelt L, Farrell DP, White SR, Woodsmith J, Svetlov V, Goldstein JS, Nager AR, Li Z, Muller J, Dollfus H, Nudler E, Stelzl U, DiMaio F, Nachury MV, Walz T (2019) The Molecular Architecture of Native BBSome Obtained by an Integrated Structural Approach. Structure 27:1384–1394 e1384. doi:10.1016/j.str.2019.06.006 [PubMed: 31303482]
35. Civitci F, Shangguan J, Zheng T, Tao K, Rames M, Kenison J, Zhang Y, Wu L, Phelps C, Esener S, Nan X (2020) Fast and multiplexed superresolution imaging with DNA-PAINTERS. Nat Commun 11:4339. doi:10.1038/s41467-020-18181-6 [PubMed: 32859909]
36. Cohen AI (1960) The ultrastructure of the rods of the mouse retina. Am J Anat 107:23–48. doi:10.1002/aja.1001070103 [PubMed: 13694328]
37. Conkar D, Culfa E, Odabasi E, Rauniyar N, Yates JR, Firat-Karalar EN 3rd (2017) The centriolar satellite protein CCDC66 interacts with CEP290 and functions in cilium formation and trafficking. J Cell Sci 130:1450–1462. doi:10.1242/jcs.196832 [PubMed: 28235840]
38. Craige B, Tsao C-C, Diener DR, Hou Y, Lechtreck K-F, Rosenbaum JL, Witman GB (2010) CEP290 tethers flagellar transition zone microtubules to the membrane and regulates flagellar protein content. J Cell Biol 190:927–940. doi:10.1083/jcb.201006105 [PubMed: 20819941]
39. Craige B, Tsao CC, Diener DR, Hou Y, Lechtreck KF, Rosenbaum JL, Witman GB (2010) CEP290 tethers flagellar transition zone microtubules to the membrane and regulates flagellar protein content. J Cell Biol 190:927–940 [PubMed: 20819941]
40. Devi R, Pelletier L, Prosser SL (2020) Charting the complex composite nature of centrosomes, primary cilia and centriolar satellites. Curr Opin Struct Biol 66:32–40. doi:10.1016/j.sbi.2020.10.006 [PubMed: 33130249]
41. Dharmat R, Eblimit A, Robichaux MA, Zhang Z, Nguyen TT, Jung SY, He F, Jain A, Li Y, Qin J, Overbeek P, Roepman R, Mardon G, Wensel TG, Chen R (2018) SPATA7 maintains a novel photoreceptor-specific zone in the distal connecting cilium. J Cell Biol 217:2851–2865. doi:10.1083/jcb.201712117 [PubMed: 29899041]
42. Ding JD, Salinas RY, Arshavsky VY (2015) Discs of mammalian rod photoreceptors form through the membrane evagination mechanism. J Cell Biol 211:495–502. doi:10.1083/jcb.201508093 [PubMed: 26527746]
43. Downing KH, Sui H (2007) Structural insights into microtubule doublet interactions in axonemes. Curr Opin Struct Biol 17:253–259 [PubMed: 17387011]
44. Evans RJ, Schwarz N, Nagel-Wolfrum K, Wolfrum U, Hardcastle AJ, Cheetham ME (2010) The retinitis pigmentosa protein RP2 links pericentriolar vesicle transport between the Golgi and the primary cilium. Hum Mol Genet 19:1358–1367. doi:10.1093/hmg/ddq012 [PubMed: 20106869]
45. Falk N, Joachimsthaler A, Kessler K, Lux UT, Noegel AA, Kremers J, Brandstatter JH, Giessl A, Falk N, Joachimsthaler A, Kessler K, Lux UT, Noegel AA, Kremers J, Brandstatter JH, Giessl A (2019) Lack of a Retinal Phenotype in a Syne-2/Nesprin-2 Knockout Mouse Model. Cells 8. doi:10.3390/cells8101238
46. Fansa EK, Wittinghofer A (2016) Sorting of lipidated cargo by the Arl2/Arl3 system. Small GTPases 7:222–230. doi:10.1080/21541248.2016.1224454 [PubMed: 27806215]
47. Fariss RN, Molday RS, Fisher SK, Matsumoto B (1997) Evidence from normal and degenerating photoreceptors that two outer segment integral membrane proteins have separate transport pathways. J Comp Neurol 387:148–156. [PubMed: 9331178]
48. Fernandez JJ, Li S, Agard DA (2019) Consideration of sample motion in cryo-tomography based on alignment residual interpolation. J Struct Biol 205:1–6. doi:10.1016/j.jsb.2019.01.005
49. Fernandez JJ, Li S, Bharat TAM, Agard DA (2018) Cryo-tomography tilt-series alignment with consideration of the beam-induced sample motion. J Struct Biol 202:200–209. doi:10.1016/j.jsb.2018.02.001 [PubMed: 29410148]
50. Frederick JM, Hanke-Gogokhia C, Ying G, Baehr W (2020) Diffuse or hitch a ride: how photoreceptor lipidated proteins get from here to there. Biol Chem 401:573–584. doi:10.1515/hsz-2019-0375 [PubMed: 31811799]
51. Galaz-Montoya JG, Ludtke SJ (2017) The advent of structural biology in situ by single particle cryo-electron tomography. Biophys Rep 3:17–35. doi:10.1007/s41048-017-0040-0 [PubMed: 28781998]

52. Gambarotto D, Zwettler FU, Le Guennec M, Schmidt-Cernohorska M, Fortun D, Borgers S, Heine J, Schloetel JG, Reuss M, Unser M, Boyden ES, Sauer M, Hamel V, Guichard P (2019) Imaging cellular ultrastructures using expansion microscopy (U-ExM). Nat Methods 16:71–74. doi:10.1038/s41592-018-0238-1 [PubMed: 30559430]

53. Gao M, Maraspini R, Beutel O, Zehtabian A, Eickholt B, Honigmann A, Ewers H (2018) Expansion Stimulated Emission Depletion Microscopy (ExSTED). ACS Nano 12:4178–4185. doi:10.1021/acsnano.8b00776 [PubMed: 29672025]

54. Garcia G, Raleigh DR 3rd, Reiter JF (2018) How the Ciliary Membrane Is Organized Inside-Out to Communicate Outside-In. Curr Biol 28:R421–R434. doi:10.1016/j.cub.2018.03.010 [PubMed: 29689227]

55. Gheiratmand L, Coyaud E, Gupta GD, Laurent EM, Hasegan M, Prosser SL, Goncalves J, Raught B, Pelletier L (2019) Spatial and proteomic profiling reveals centrosome-independent features of centriolar satellites. EMBO J 38:e101109. doi:10.15252/embj.2018101109 [PubMed: 31304627]

56. Ghossoub R, Molla-Herman A, Bastin P, Benmerah A (2011) The ciliary pocket: a once-forgotten membrane domain at the base of cilia. Biol Cell 103:131–144. doi:10.1042/BC20100128 [PubMed: 21275905]

57. Gibbons IR (1961) The relationship between the fine structure and direction of beat in gill cilia of a lamellibranch mollusc. J Biophys Biochem Cytol 11:179–205. doi:10.1083/jcb.11.1.179 [PubMed: 13898346]

58. Gilliam JC, Chang JT, Sandoval IM, Zhang Y, Li T, Pittler SJ, Chiu W, Wensel TG (2012) Three-dimensional architecture of the rod sensory cilium and its disruption in retinal neurodegeneration. Cell 151:1029–1041. doi:10.1016/j.cell.2012.10.038 S0092-8674(12)01301-3 [pii] [PubMed: 23178122]

59. Gilula NB, Satir P (1972) The ciliary necklace. A ciliary membrane specialization. J Cell Biol 53:494–509. doi:10.1083/jcb.53.2.494 [PubMed: 4554367]

60. Gogendeau D, Lemullois M, Le Borgne P, Castelli M, Aubusson-Fleury A, Arnaiz O, Cohen J, Vesque C, Schneider-Maunoury S, Bouhouche K, Koll F, Tassin AM (2020) MKS-NPHP module proteins control ciliary shedding at the transition zone. PLoS Biol 18:e3000640. doi:10.1371/journal.pbio.3000640 [PubMed: 32163404]

61. Gomez-Garcia PA, Garbacik ET, Otterstrom JJ, Garcia-Parajo MF, Lakadamyali M (2018) Excitation-multiplexed multicolor superresolution imaging with fm-STORM and fm-DNA-PAINT. Proc Natl Acad Sci U S A 115:12991–12996. doi:10.1073/pnas.1804725115 [PubMed: 30509979]

62. Greenan GA, Keszthelyi B, Vale RD, Agard DA (2018) Insights into centriole geometry revealed by cryotomography of doublet and triplet centrioles. Elife 7. doi:10.7554/eLife.36851

63. Greenan GA, Vale RD, Agard DA (2020) Electron cryotomography of intact motile cilia defines the basal body to axoneme transition. J Cell Biol 219. doi:10.1083/jcb.201907060

64. Greiner JV, Weidman TA, Bodley HD, Greiner CA (1981) Ciliogenesis in photoreceptor cells of the retina. Exp Eye Res 33:433–446 [PubMed: 7297621]

65. Gross OP, Pugh EN, Jr., Burns ME (2012) Spatiotemporal cGMP dynamics in living mouse rods. Biophys J 102:1775–1784. doi:10.1016/j.bpj.2012.03.035 S0006-3495(12)00346-3 [pii] [PubMed: 22768933]

66. Gustafsson MG, Shao L, Carlton PM, Wang CJ, Golubovskaya IN, Cande WZ, Agard DA, Sedat JW (2008) Three-dimensional resolution doubling in wide-field fluorescence microscopy by structured illumination. Biophys J 94:4957–4970. doi:10.1529/biophysj.107.120345 [PubMed: 18326650]

67. Hanke-Gogokhia C, Zhang H, Frederick JM, Baehr W (2016) The Function of Arf-like Proteins ARL2 and ARL3 in Photoreceptors. Adv Exp Med Biol 854:655–661. doi:10.1007/978-3-319-17121-0_87 [PubMed: 26427472]

68. Hendrickson A, Bumsted-O'Brien K, Natoli R, Ramamurthy V, Possin D, Provis J (2008) Rod photoreceptor differentiation in fetal and infant human retina. Exp Eye Res 87:415–426. doi:10.1016/j.exer.2008.07.016 [PubMed: 18778702]

69. Heuser T, Barber CF, Lin J, Krell J, Rebesco M, Porter ME, Nicastro D (2012) Cryoelectron tomography reveals doublet-specific structures and unique interactions in the I1 dynein. Proc Natl

Acad Sci U S A 109:E2067–2076. doi:10.1073/pnas.1120690109 1120690109 [pii] [PubMed: 22733763]

70. Hori A, Toda T (2017) Regulation of centriolar satellite integrity and its physiology. Cell Mol Life Sci 74:213–229. doi:10.1007/s00018-016-2315-x [PubMed: 27484406]
71. Horst CJ, Forestner DM, Besharse JC (1987) Cytoskeletal-membrane interactions: a stable interaction between cell surface glycoconjugates and doublet microtubules of the photoreceptor connecting cilium. J Cell Biol 105:2973–2987 [PubMed: 3693403]
72. Huang B, Babcock H, Zhuang X (2010) Breaking the diffraction barrier: super-resolution imaging of cells. Cell 143:1047–1058. doi:10.1016/j.cell.2010.12.002 S0092-8674(10)01420-0 [pii] [PubMed: 21168201]
73. Huang XF, Xiang L, Fang XL, Liu WQ, Zhuang YY, Chen ZJ, Shen RJ, Cheng W, Han RY, Zheng SS, Chen XJ, Liu X, Jin ZB (2019) Functional characterization of CEP250 variant identified in nonsyndromic retinitis pigmentosa. Hum Mutat 40:1039–1045. doi:10.1002/humu.23759 [PubMed: 30998843]
74. Humbert MC, Weihbrecht K, Searby CC, Li Y, Pope RM, Sheffield VC, Seo S (2012) ARL13B, PDE6D, and CEP164 form a functional network for INPP5E ciliary targeting. Proc Natl Acad Sci U S A 109:19691–19696. doi:10.1073/pnas.1210916109 [PubMed: 23150559]
75. Iannaccone A, Man D, Waseem N, Jennings BJ, Ganapathiraju M, Gallaher K, Reese E, Bhattacharya SS, Klein-Seetharaman J (2006) Retinitis pigmentosa associated with rhodopsin mutations: Correlation between phenotypic variability and molecular effects. Vision Res 46:4556–4567. doi:10.1016/j.visres.2006.08.018 [PubMed: 17014888]
76. Ikeda K, Ikeda T, Morikawa K, Kamiya R (2007) Axonemal localization of Chlamydomonas PACRG, a homologue of the human Parkin-coregulated gene product. Cell Motil Cytoskeleton 64:814–821. doi:10.1002/cm.20225 [PubMed: 17654607]
77. Imanishi Y (2019) Protein Sorting in Healthy and Diseased Photoreceptors. Annu Rev Vis Sci. doi:10.1146/annurev-vision-091718-014843
78. Imanishi Y, Palczewski K (2010) Visualization of retinoid storage and trafficking by two-photon microscopy. Methods Mol Biol 652:247–261. doi:10.1007/978-1-60327-325-1_14 [PubMed: 20552433]
79. Insinna C, Besharse JC (2008) Intraflagellar transport and the sensory outer segment of vertebrate photoreceptors. Dev Dyn 237:1982–1992. doi:10.1002/dvdy.21554 [PubMed: 18489002]
80. Insinna C, Pathak N, Perkins B, Drummond I, Besharse JC (2008) The homodimeric kinesin, Kif17, is essential for vertebrate photoreceptor sensory outer segment development. Developmental biology 316:160–170. doi:10.1016/j.ydbio.2008.01.025 [PubMed: 18304522]
81. Ishikawa H, Kubo A, Tsukita S, Tsukita S (2005) Odf2-deficient mother centrioles lack distal/subdistal appendages and the ability to generate primary cilia. Nat Cell Biol 7:517–524. doi:10.1038/ncb1251 [PubMed: 15852003]
82. Jana SC, Mendonca S, Machado P, Werner S, Rocha J, Pereira A, Maiato H, Bettencourt-Dias M (2018) Differential regulation of transition zone and centriole proteins contributes to ciliary base diversity. Nat Cell Biol 20:928–941. doi:10.1038/s41556-018-0132-1 [PubMed: 30013109]
83. Jaulin F, Kreitzer G (2010) KIF17 stabilizes microtubules and contributes to epithelial morphogenesis by acting at MT plus ends with EB1 and APC. J Cell Biol 190:443–460. doi:10.1083/jcb.201006044 [PubMed: 20696710]
84. Jiang L, Wei Y, Ronquillo CC, Marc RE, Yoder BK, Frederick JM, Baehr W (2015) Heterotrimeric kinesin-2 (KIF3) mediates transition zone and axoneme formation of mouse photoreceptors. J Biol Chem 290:12765–12778. doi:10.1074/jbc.M115.638437 [PubMed: 25825494]
85. Johnson CA, Malicki JJ (2019) The Nuclear Arsenal of Cilia. Dev Cell 49:161–170. doi:10.1016/j.devcel.2019.03.009 [PubMed: 31014478]
86. Jordan MA, Diener DR, Stepanek L, Pigino G (2018) The cryo-EM structure of intraflagellar transport trains reveals how dynein is inactivated to ensure unidirectional anterograde movement in cilia. Nat Cell Biol 20:1250–1255. doi:10.1038/s41556-018-0213-1 [PubMed: 30323187]
87. Jordan MA, Pigino G (2019) In situ cryo-electron tomography and subtomogram averaging of intraflagellar transport trains. Methods Cell Biol 152:179–195. doi:10.1016/bs.mcb.2019.04.005 [PubMed: 31326020]

88. Katoh Y, Chiba S, Nakayama K (2020) Practical method for superresolution imaging of primary cilia and centrioles by expansion microscopy using an amplibody for fluorescence signal amplification. Mol Biol Cell 31:2195–2206. doi:10.1091/mbc.E20-040-250 [PubMed: 32726175]

89. Katoh Y, Nozaki S, Hartanto D, Miyano R, Nakayama K (2015) Architectures of multisubunit complexes revealed by a visible immunoprecipitation assay using fluorescent fusion proteins. J Cell Sci 128:2351–2362. doi:10.1242/jcs.168740 [PubMed: 25964651]

90. Kee HL, Dishinger JF, Blasius TL, Liu CJ, Margolis B, Verhey KJ (2012) A size-exclusion permeability barrier and nucleoporins characterize a ciliary pore complex that regulates transport into cilia. Nat Cell Biol 14:431–437. doi:10.1038/ncb2450 [PubMed: 22388888]

91. Khanna H (2018) More Than Meets the Eye: Current Understanding of RPGR Function. Adv Exp Med Biol 1074:521–538. doi:10.1007/978-3-319-75402-4_64 [PubMed: 29721984]

92. Kim J, Krishnaswami SR, Gleeson JG (2008) CEP290 interacts with the centriolar satellite component PCM-1 and is required for Rab8 localization to the primary cilium. Hum Mol Genet 17:3796–3805 [PubMed: 18772192]

93. Kim JC, Badano JL, Sibold S, Esmail MA, Hill J, Hoskins BE, Leitch CC, Venner K, Ansley SJ, Ross AJ, Leroux MR, Katsanis N, Beales PL (2004) The Bardet-Biedl protein BBS4 targets cargo to the pericentriolar region and is required for microtubule anchoring and cell cycle progression. Nat Genet 36:462–470. doi:10.1038/ng1352 [PubMed: 15107855]

94. Klinger M, Wang W, Kuhns S, Barenz F, Drager-Meurer S, Pereira G, Gruss OJ (2014) The novel centriolar satellite protein SSX2IP targets Cep290 to the ciliary transition zone. Mol Biol Cell 25:495–507. doi:10.1091/mbc.E13-09-0526 [PubMed: 24356449]

95. Knabe W, Kuhn H (1997) Ciliogenesis in photoreceptor cells of the tree shrew retina. Anat Embryol (Berl) 196:123–131

96. Kong D, Sahabandu N, Sullenberger C, Vásquez-Limeta A, Luvsanjav D, Lukasik K, Loncarek J (2020) Prolonged mitosis results in structurally aberrant and over-elongated centrioles. J Cell Biol 219. doi:10.1083/jcb.201910019

97. Koyfman AY, Schmid MF, Gheiratmand L, Fu CJ, Khant HA, Huang D, He CY, Chiu W (2011) Structure of Trypanosoma brucei flagellum accounts for its bihelical motion. Proc Natl Acad Sci U S A 108:11105–11108. doi:1103634108 [pii] 10.1073/pnas.1103634108 [PubMed: 21690369]

98. Krock BL, Mills-Henry I, Perkins BD (2009) Retrograde intraflagellar transport by cytoplasmic dynein-2 is required for outer segment extension in vertebrate photoreceptors but not arrestin translocation. Invest Ophthalmol Vis Sci 50:5463–5471. doi:10.1167/iovs.09-3828 iovs.09-3828 [pii] [PubMed: 19474410]

99. Kubo A, Sasaki H, Yuba-Kubo A, Tsukita S, Shiina N (1999) Centriolar satellites: molecular characterization, ATP-dependent movement toward centrioles and possible involvement in ciliogenesis. J Cell Biol 147:969–980. doi:10.1083/jcb.147.5.969 [PubMed: 10579718]

100. Kurner J, Medalia O, Linaroudis AA, Baumeister W (2004) New insights into the structural organization of eukaryotic and prokaryotic cytoskeletons using cryo-electron tomography. Exp Cell Res 301:38–42 [PubMed: 15501443]

101. Lakadamyali M, Babcock H, Bates M, Zhuang X, Lichtman J (2012) 3D multicolor super-resolution imaging offers improved accuracy in neuron tracing. PLoS ONE 7:e30826. doi:10.1371/journal.pone.0030826 PONE-D-11-17942 [pii] [PubMed: 22292051]

102. LaVail MM (1973) Kinetics of rod outer segment renewal in the developing mouse retina. J Cell Biol 58:650–661. doi:10.1083/jcb.58.3.650 [PubMed: 4747920]

103. Le Guennec M, Klena N, Gambarotto D, Laporte MH, Tassin AM, van den Hoek H, Erdmann PS, Schaffer M, Kovacik L, Borgers S, Goldie KN, Stahlberg H, Bornens M, Azimzadeh J, Engel BD, Hamel V, Guichard P (2020) A helical inner scaffold provides a structural basis for centriole cohesion. Sci Adv 6:eaaz4137. doi:10.1126/sciadv.aaz4137 [PubMed: 32110738]

104. Leigh KE, Navarro PP, Scaramuzza S, Chen W, Zhang Y, Castano-Diez D, Kudryashev M (2019) Subtomogram averaging from cryo-electron tomograms. Methods Cell Biol 152:217–259. doi:10.1016/bs.mcb.2019.04.003 [PubMed: 31326022]

105. Lewis TR, Zareba M, Link BA, Besharse JC (2018) Cone myoid elongation involves unidirectional microtubule movement mediated by dynein-1. Mol Biol Cell 29:180–190. doi:10.1091/mbc.E17-08-0525 [PubMed: 29142075]

106. Li S, Fernandez JJ, Marshall WF, Agard DA (2012) Three-dimensional structure of basal body triplet revealed by electron cryo-tomography. Embo J 31:552–562. doi:10.1038/emboj.2011.460 emboj2011460 [pii] [PubMed: 22157822]

107. Linck R, Fu X, Lin J, Ouch C, Schefter A, Steffen W, Warren P, Nicastro D (2014) Insights into the structure and function of ciliary and flagellar doublet microtubules: tektins, Ca2+-binding proteins, and stable protofilaments. J Biol Chem 289:17427–17444. doi:10.1074/jbc.M114.568949 [PubMed: 24794867]

108. Lodowski KH, Imanishi Y (2015) Monitoring of rhodopsin trafficking and mistrafficking in live photoreceptors. Methods Mol Biol 1271:293–307. doi:10.1007/978-1-4939-2330-4_19 [PubMed: 25697531]

109. Ludlam WG, Aoba T, Cuellar J, Bueno-Carrasco MT, Makaju A, Moody JD, Franklin S, Valpuesta JM, Willardson BM (2019) Molecular architecture of the Bardet-Biedl syndrome protein 2-7-9 subcomplex. J Biol Chem 294:16385–16399. doi:10.1074/jbc.RA119.010150 [PubMed: 31530639]

110. Lyubarsky AL, Daniele LL, Pugh EN, Jr. (2004) From candelas to photoisomerizations in the mouse eye by rhodopsin bleaching in situ and the light-rearing dependence of the major components of the mouse ERG. Vision Res 44:3235–3251 [PubMed: 15535992]

111. Maerker T, van Wijk E, Overlack N, Kersten FF, McGee J, Goldmann T, Sehn E, Roepman R, Walsh EJ, Kremer H, Wolfrum U (2008) A novel Usher protein network at the periciliary reloading point between molecular transport machineries in vertebrate photoreceptor cells. Hum Mol Genet 17:71–86. doi:ddm285 [pii] 10.1093/hmg/ddm285 [PubMed: 17906286]

112. Mahecic D, Gambarotto D, Douglass KM, Fortun D, Banterle N, Ibrahim KA, Le Guennec M, Gönczy P, Hamel V, Guichard P, Manley S (2020) Homogeneous multifocal excitation for high-throughput super-resolution imaging. Nat Methods 17:726–733. doi:10.1038/s41592-020-0859-z [PubMed: 32572233]

113. Malinski JA, Wensel TG (1992) Membrane stimulation of cGMP phosphodiesterase activation by transducin: comparison of phospholipid bilayers to rod outer segment membranes. Biochemistry 31:9502–9512 [PubMed: 1327116]

114. May-Simera H, Nagel-Wolfrum K, Wolfrum U (2017) Cilia - The sensory antennae in the eye. Prog Retin Eye Res 60:144–180. doi:10.1016/j.preteyeres.2017.05.001 [PubMed: 28504201]

115. McEwen BF, Frank J (2001) Electron tomographic and other approaches for imaging molecular machines. Curr Opin Neurobiol 11:594–600 [PubMed: 11595494]

116. McIntosh R, Nicastro D, Mastronarde D (2005) New views of cells in 3D: an introduction to electron tomography. Trends Cell Biol 15:43–51. doi:10.1016/j.tcb.2004.11.009 [PubMed: 15653077]

117. Megaw R, Mellough C, Wright A, Lako M, Ffrench-Constant C (2015) Use of induced pluripotent stem-cell technology to understand photoreceptor cytoskeletal dynamics in retinitis pigmentosa. Lancet 385 Suppl 1:S69. doi:10.1016/S0140-6736(15)60384-1

118. Mohan S, Timbers TA, Kennedy J, Blacque OE, Leroux MR (2013) Striated rootlet and nonfilamentous forms of rootletin maintain ciliary function. Curr Biol 23:2016–2022. doi:10.1016/j.cub.2013.08.033 [PubMed: 24094853]

119. Molday RS, Hicks D, Molday L (1987) Peripherin. A rim-specific membrane protein of rod outer segment discs. Invest Ophthalmol Vis Sci 28:50–61. [PubMed: 2433249]

120. Molla-Herman A, Ghossoub R, Blisnick T, Meunier A, Serres C, Silbermann F, Emmerson C, Romeo K, Bourdoncle P, Schmitt A, Saunier S, Spassky N, Bastin P, Benmerah A (2010) The ciliary pocket: an endocytic membrane domain at the base of primary and motile cilia. J Cell Sci 123:1785–1795. doi:10.1242/jcs.059519 [PubMed: 20427320]

121. Moritz M, Braunfeld MB, Sedat JW, Alberts B, Agard DA (1995) Microtubule nucleation by gamma-tubulin-containing rings in the centrosome. Nature 378:638–640. doi:10.1038/378638a0 [PubMed: 8524401]

122. Moritz OL, Molday RS (1996) Molecular cloning, membrane topology, and localization of bovine rom-1 in rod and cone photoreceptor cells. Invest Ophthalmol Vis Sci 37:352–362. [PubMed: 8603840]

123. Moye AR, Singh R, Kimler VA, Dilan TL, Munezero D, Saravanan T, Goldberg AFX, Ramamurthy V (2018) ARL2BP, a protein linked to Retinitis Pigmentosa, is needed for normal photoreceptor cilia doublets and outer segment structure. Mol Biol Cell:mbcE. doi:10.1091/mbc.E18-01-0040 [PubMed: 18010040]

124. Muhlhans J, Brandstatter JH, Giessl A (2011) The centrosomal protein pericentrin identified at the basal body complex of the connecting cilium in mouse photoreceptors. PLoS One 6:e26496. doi:10.1371/journal.pone.0026496 [PubMed: 22031837]

125. Muresan V, Besharse JC (1994) Complex intermolecular interactions maintain a stable linkage between the photoreceptor connecting cilium axoneme and plasma membrane. Cell Motil Cytoskeleton 28:213–230. doi:10.1002/cm.970280305 [PubMed: 7954850]

126. Muresan V, Joshi HC, Besharse JC (1993) Gamma-tubulin in differentiated cell types: localization in the vicinity of basal bodies in retinal photoreceptors and ciliated epithelia. J Cell Sci 104 (Pt 4):1229–1237 [PubMed: 7686172]

127. Murga-Zamalloa CA, Desai NJ, Hildebrandt F, Khanna H (2010) Interaction of ciliary disease protein retinitis pigmentosa GTPase regulator with nephronophthisis-associated proteins in mammalian retinas. Mol Vis 16:1373–1381. doi:151 [pii] [PubMed: 20664800]

128. Murga-Zamalloa CA, Swaroop A, Khanna H (2009) RPGR-containing protein complexes in syndromic and non-syndromic retinal degeneration due to ciliary dysfunction. J Genet 88:399–407 [PubMed: 20090203]

129. Mustafi D, Engel AH, Palczewski K (2009) Structure of cone photoreceptors. Prog Retin Eye Res 28:289–302. doi:10.1016/j.preteyeres.2009.05.003 [PubMed: 19501669]

130. Nachury M, Seeley E, Jin H (2010) Trafficking to the ciliary membrane: how to get across the periciliary diffusion barrier? Annu Rev Cell Dev Bio 26:59–87. doi:10.1146/annurev.cellbio.042308.113337 [PubMed: 19575670]

131. Nachury MV (2018) The molecular machines that traffic signaling receptors into and out of cilia. Curr Opin Cell Biol 51:124–131. doi:10.1016/j.ceb.2018.03.004 [PubMed: 29579578]

132. Nachury MV, Loktev AV, Zhang Q, Westlake CJ, Peranen J, Merdes A, Slusarski DC, Scheller RH, Bazan JF, Sheffield VC, Jackson PK (2007) A core complex of BBS proteins cooperates with the GTPase Rab8 to promote ciliary membrane biogenesis. Cell 129:1201–1213 [PubMed: 17574030]

133. Najafi M, Calvert PD (2015) Measurements of rhodopsin diffusion within signaling membrane microcompartments in live photoreceptors. Methods Mol Biol 1271:309–323. doi:10.1007/978-1-4939-2330-4_20 [PubMed: 25697532]

134. Nakayama K, Katoh Y (2018) Ciliary protein trafficking mediated by IFT and BBSome complexes with the aid of kinesin-2 and dynein-2 motors. J Biochem 163:155–164. doi:10.1093/jb/mvx087 [PubMed: 29272450]

135. Nicastro D (2009) Cryo-electron microscope tomography to study axonemal organization. Methods Cell Biol 91:1–39. doi:S0091-679X(08)91001-3 [pii] 10.1016/S0091-679X(08)91001-3 [PubMed: 20409778]

136. Nicastro D, Fu X, Heuser T, Tso A, Porter ME, Linck RW (2011) Cryo-electron tomography reveals conserved features of doublet microtubules in flagella. Proceedings of the National Academy of Sciences of the United States of America 108:E845–E853. doi:10.1073/pnas.1106178108 [PubMed: 21930914]

137. Nicastro D, Schwartz C, Pierson J, Gaudette R, Porter ME, McIntosh JR (2006) The molecular architecture of axonemes revealed by cryoelectron tomography. Science 313:944–948. doi:10.1126/science.1128618 [PubMed: 16917055]

138. Nickell S, Park PS, Baumeister W, Palczewski K (2007) Three-dimensional architecture of murine rod outer segments determined by cryoelectron tomography. J Cell Biol 177:917–925 [PubMed: 17535966]

139. Oda T, Abe T, Yanagisawa H, Kikkawa M (2016) Docking-complex-independent alignment of Chlamydomonas outer dynein arms with 24-nm periodicity in vitro. J Cell Sci 129:1547–1551. doi:10.1242/jcs.184598 [PubMed: 26933181]

140. Odabasi E, Gul S, Kavakli IH, Firat-Karalar EN (2019) Centriolar satellites are required for efficient ciliogenesis and ciliary content regulation. EMBO Rep 20. doi:10.15252/embr.201947723

141. Oikonomou CM, Jensen GJ (2017) Cellular Electron Cryotomography: Toward Structural Biology In Situ. Annu Rev Biochem 86:873–896. doi:10.1146/annurev-biochem-061516-044741 [PubMed: 28426242]

142. Otsu W, Hsu YC, Chuang JZ, Sung CH (2019) The Late Endosomal Pathway Regulates the Ciliary Targeting of Tetraspanin Protein Peripherin 2. J Neurosci 39:3376–3393. doi:10.1523/JNEUROSCI.2811-18.2019 [PubMed: 30819798]

143. Ou YY, Zhang M, Chi S, Matyas JR, Rattner JB (2003) Higher order structure of the PCM adjacent to the centriole. Cell Motil Cytoskeleton 55:125–133. doi:10.1002/cm.10115 [PubMed: 12740873]

144. Owa M, Uchihashi T, Yanagisawa HA, Yamano T, Iguchi H, Fukuzawa H, Wakabayashi KI, Ando T, Kikkawa M (2019) Inner lumen proteins stabilize doublet microtubules in cilia and flagella. Nat Commun 10:1143. doi:10.1038/s41467-019-09051-x [PubMed: 30850601]

145. Papermaster DS, Schneider BG, DeFoe D, Besharse JC (1986) Biosynthesis and vectorial transport of opsin on vesicles in retinal rod photoreceptors. J Histochem Cytochem 34:5–16. [PubMed: 2934469]

146. Pazour GJ, Baker SA, Deane JA, Cole DG, Dickert BL, Rosenbaum JL, Witman GB, Besharse JC (2002) The intraflagellar transport protein, IFT88, is essential for vertebrate photoreceptor assembly and maintenance. J Cell Biol 157:103–113. doi:10.1083/jcb.200107108 jcb.200107108 [pii] [PubMed: 11916979]

147. Pazour GJ, Rosenbaum JL (2002) Intraflagellar transport and cilia-dependent diseases. Trends Cell Biol 12:551–555 [PubMed: 12495842]

148. Pearring JN, Salinas RY, Baker SA, Arshavsky VY (2013) Protein sorting, targeting and trafficking in photoreceptor cells. Prog Retin Eye Res 36:24–51. doi:10.1016/j.preteyeres.2013.03.002 [PubMed: 23562855]

149. Pedersen LB, Rosenbaum JL (2008) Intraflagellar transport (IFT) role in ciliary assembly, resorption and signalling. Curr Top Dev Biol 85:23–61 [PubMed: 19147001]

150. Peters KR, Palade GE, Schneider BG, Papermaster DS (1983) Fine structure of a periciliary ridge complex of frog retinal rod cells revealed by ultrahigh resolution scanning electron microscopy. J Cell Biol 96:265–276. [PubMed: 6219117]

151. Pigino G, Maheshwari A, Bui KH, Shingyoji C, Kamimura S, Ishikawa T (2012) Comparative structural analysis of eukaryotic flagella and cilia from Chlamydomonas, Tetrahymena, and sea urchins. Journal of structural biology 178:199–206. doi:10.1016/j.jsb.2012.02.012 [PubMed: 22406282]

152. Prasai A, Schmidt Cernohorska M, Ruppova K, Niederlova V, Andelova M, Draber P, Stepanek O, Huranova M (2020) The BBSome assembly is spatially controlled by BBS1 and BBS4 in human cells. J Biol Chem 295:14279–14290. doi:10.1074/jbc.RA120.013905 [PubMed: 32759308]

153. Punge A, Rizzoli SO, Jahn R, Wildanger JD, Meyer L, Schonle A, Kastrup L, Hell SW (2008) 3D reconstruction of high-resolution STED microscope images. Microsc Res Tech 71:644–650. doi:10.1002/jemt.20602 [PubMed: 18512740]

154. Rattner A, Smallwood PM, Williams J, Cooke C, Savchenko A, Lyubarsky A, Pugh EN, Nathans J (2001) A photoreceptor-specific cadherin is essential for the structural integrity of the outer segment and for photoreceptor survival. Neuron 32:775–786 [PubMed: 11738025]

155. Reese TS (1965) Olfactory Cilia in the Frog. J Cell Biol 25:209–230. doi:10.1083/jcb.25.2.209 [PubMed: 19866665]

156. Ringo DL (1967) Flagellar motion and fine structure of the flagellar apparatus in Chlamydomonas. J Cell Biol 33:543–571 [PubMed: 5341020]

157. Robichaux MA, Potter VL, Zhang Z, He F, Liu J, Schmid MF, Wensel TG (2019) Defining the layers of a sensory cilium with STORM and cryoelectron nanoscopy. Proc Natl Acad Sci U S A 116:23562–23572. doi:10.1073/pnas.1902003116 [PubMed: 31690665]

158. Rohlich P (1975) The sensory cilium of retinal rods is analogous to the transitional zone of motile cilia. Cell Tissue Res 161:421–430 [PubMed: 1175211]

159. Roof DJ, Heuser JE (1982) Surfaces of rod photoreceptor disk membranes: integral membrane components. J Cell Biol 95:487–500 [PubMed: 6815210]

160. Roof DJ, Korenbrot JI, Heuser JE (1982) Surfaces of rod photoreceptor disk membranes: light-activated enzymes. J Cell Biol 95:501–509 [PubMed: 6292237]

161. Rosenbaum JL, Witman GB (2002) Intraflagellar transport. Nat Rev Mol Cell Biol 3:813–825 [PubMed: 12415299]

162. Sahabandu N, Kong D, Magidson V, Nanjundappa R, Sullenberger C, Mahjoub MR, Loncarek J (2019) Expansion microscopy for the analysis of centrioles and cilia. J Microsc 276:145–159. doi:10.1111/jmi.12841 [PubMed: 31691972]

163. Saka SK, Wang Y, Kishi JY, Zhu A, Zeng Y, Xie W, Kirli K, Yapp C, Cicconet M, Beliveau BJ, Lapan SW, Yin S, Lin M, Boyden ES, Kaeser PS, Pihan G, Church GM, Yin P (2019) Immuno-SABER enables highly multiplexed and amplified protein imaging in tissues. Nat Biotechnol 37:1080–1090. doi:10.1038/s41587-019-0207-y [PubMed: 31427819]

164. Salisbury JL (1995) Centrin, centrosomes, and mitotic spindle poles. Curr Opin Cell Biol 7:39–45. doi:10.1016/0955-0674(95)80043-3 [PubMed: 7755988]

165. Sanchez RM, Zhang Y, Chen W, Dietrich L, Kudryashev M (2020) Subnanometer-resolution structure determination in situ by hybrid subtomogram averaging - single particle cryo-EM. Nat Commun 11:3709. doi:10.1038/s41467-020-17466-0 [PubMed: 32709843]

166. Schaffer M, Pfeffer S, Mahamid J, Kleindiek S, Laugks T, Albert S, Engel BD, Rummel A, Smith AJ, Baumeister W, Plitzko JM (2019) A cryo-FIB lift-out technique enables molecular-resolution cryo-ET within native Caenorhabditis elegans tissue. Nat Methods 16:757–762. doi:10.1038/s41592-019-0497-5 [PubMed: 31363205]

167. Scholey JM (2008) Intraflagellar transport motors in cilia: moving along the cell's antenna. J Cell Biol 180:23–29 [PubMed: 18180368]

168. Schur FK (2019) Toward high-resolution in situ structural biology with cryo-electron tomography and subtomogram averaging. Curr Opin Struct Biol 58:1–9. doi:10.1016/j.sbi.2019.03.018 [PubMed: 31005754]

169. Sedmak T, Wolfrum U (2010) Intraflagellar transport molecules in ciliary and nonciliary cells of the retina. J Cell Biol 189:171–186. doi:10.1083/jcb.200911095 jcb.200911095 [pii] [PubMed: 20368623]

170. Sedmak T, Wolfrum U (2011) Intraflagellar transport proteins in ciliogenesis of photoreceptor cells. Biol Cell 103:449–466. doi:10.1042/BC20110034 BC20110034 [pii] [PubMed: 21732910]

171. Seo S, Datta P (2017) Photoreceptor outer segment as a sink for membrane proteins: hypothesis and implications in retinal ciliopathies. Hum Mol Genet 26:R75–R82. doi:10.1093/hmg/ddx163 [PubMed: 28453661]

172. Shi X, Chen M, Yu Z, Bell JM, Wang H, Forrester I, Villarreal H, Jakana J, Du D, Luisi BF, Ludtke SJ, Wang Z (2019) In situ structure and assembly of the multidrug efflux pump AcrAB-TolC. Nat Commun 10:2635. doi:10.1038/s41467-019-10512-6 [PubMed: 31201302]

173. Shiba D, Yokoyama T (2012) The ciliary transitional zone and nephrocystins. Differentiation 83:S91–96. doi:10.1016/j.diff.2011.11.006 [PubMed: 22169048]

174. Singh SK, Gui M, Koh F, Yip MC, Brown A (2020) Structure and activation mechanism of the BBSome membrane protein trafficking complex. Elife 9. doi:10.7554/eLife.53322

175. Sjostrand FS (1953) The ultrastructure of the innersegments of the retinal rods of the guinea pig eye as revealed by electron microscopy. J Cell Physiol 42:45–70

176. Smith TS, Spitzbarth B, Li J, Dugger DR, Stern-Schneider G, Sehn E, Bolch SN, McDowell JH, Tipton J, Wolfrum U, Smith WC (2013) Light-dependent phosphorylation of Bardet-Biedl syndrome 5 in photoreceptor cells modulates its interaction with arrestin1. Cell Mol Life Sci 70:4603–4616. doi:10.1007/s00018-013-1403-4 [PubMed: 23817741]

177. Snow JJ, Ou G, Gunnarson AL, Walker MR, Zhou HM, Brust-Mascher I, Scholey JM (2004) Two anterograde intraflagellar transport motors cooperate to build sensory cilia on C. elegans neurons. Nat Cell Biol 6:1109–1113. doi:10.1038/ncb1186 [PubMed: 15489852]

178. Sorokin S (1962) Centrioles and the formation of rudimentary cilia by fibroblasts and smooth muscle cells. J Cell Biol 15:363–377. doi:10.1083/jcb.15.2.363 [PubMed: 13978319]

179. Sorokin SP (1968) Reconstructions of centriole formation and ciliogenesis in mammalian lungs. J Cell Sci 3:207–230 [PubMed: 5661997]

180. Spencer WJ, Lewis TR, Pearring JN, Arshavsky VY (2020) Photoreceptor Discs: Built Like Ectosomes. Trends Cell Biol 30:904–915. doi:10.1016/j.tcb.2020.08.005 [PubMed: 32900570]

181. Spencer WJ, Lewis TR, Phan S, Cady MA, Serebrovskaya EO, Schneider NF, Kim KY, Cameron LA, Skiba NP, Ellisman MH, Arshavsky VY (2019) Photoreceptor disc membranes are formed through an Arp2/3-dependent lamellipodium-like mechanism. Proc Natl Acad Sci U S A. doi:10.1073/pnas.1913518117

182. Spira AW, Milman GE (1979) The structure and distribution of the cross-striated fibril and associated membranes in guinea pig photoreceptors. Am J Anat 155:319–337. doi:10.1002/aja.1001550304 [PubMed: 573060]

183. Spitznas M, Hogan MJ (1970) Outer segments of photoreceptors and the retinal pigment epithelium. Interrelationship in the human eye. Arch Ophthalmol 84:810–819. doi:10.1001/archopht.1970.00990040812022 [PubMed: 4321117]

184. Steib E, Laporte MH, Gambarotto D, Olieric N, Zheng C, Borgers S, Olieric V, Le Guennec M, Koll F, Tassin AM, Steinmetz MO, Guichard P, Hamel V (2020) WDR90 is a centriolar microtubule wall protein important for centriole architecture integrity. Elife 9. doi:10.7554/eLife.57205

185. Steinberg R, Wood I (1975) Clefts and microtubules of photoreceptor outer segments in the retina of the domestic cat. J Ultrastructural Res 51:397–403

186. Stowe TR, Wilkinson CJ, Iqbal A, Stearns T (2012) The centriolar satellite proteins Cep72 and Cep290 interact and are required for recruitment of BBS proteins to the cilium. Mol Biol Cell 23:3322–3335. doi:10.1091/mbc.E12-02-0134 [PubMed: 22767577]

187. Sui H, Downing KH (2006) Molecular architecture of axonemal microtubule doublets revealed by cryo-electron tomography. Nature 442:475–478. doi:nature04816 [pii] 10.1038/nature04816 [PubMed: 16738547]

188. Sun Q, Picascia T, Khan AUM, Brenna C, Heuveline V, Schmaus A, Sleeman JP, Gretz N (2020) Application of ethyl cinnamate based optical tissue clearing and expansion microscopy combined with retrograde perfusion for 3D lung imaging. Exp Lung Res:1–16. doi:10.1080/01902148.2020.1829183

189. Sun S, Fisher RL, Bowser SS, Pentecost BT, Sui H (2019) Three-dimensional architecture of epithelial primary cilia. Proc Natl Acad Sci U S A 116:9370–9379. doi:10.1073/pnas.1821064116 [PubMed: 31004057]

190. Sung C-H, Chuang J-Z (2010) The cell biology of vision. The Journal of cell biology 190:953–963. doi:10.1083/jcb.201006020

191. Tai AW, Chuang JZ, Bode C, Wolfrum U, Sung CH (1999) Rhodopsin's carboxy-terminal cytoplasmic tail acts as a membrane receptor for cytoplasmic dynein by binding to the dynein light chain Tctex-1. Cell 97:877–887 [PubMed: 10399916]

192. Takao D, Dishinger JF, Kee HL, Pinskey JM, Allen BL, Verhey KJ (2014) An assay for clogging the ciliary pore complex distinguishes mechanisms of cytosolic and membrane protein entry. Curr Biol 24:2288–2294. doi:10.1016/j.cub.2014.08.012 [PubMed: 25264252]

193. Takao D, Verhey KJ (2016) Gated entry into the ciliary compartment. Cell Mol Life Sci 73:119–127. doi:10.1007/s00018-015-2058-0 [PubMed: 26472341]

194. Takao D, Wang L, Boss A, Verhey KJ (2017) Protein Interaction Analysis Provides a Map of the Spatial and Temporal Organization of the Ciliary Gating Zone. Curr Biol 27:2296–2306 e2293. doi:10.1016/j.cub.2017.06.044 [PubMed: 28736169]

195. Tanos BE, Yang HJ, Soni R, Wang WJ, Macaluso FP, Asara JM, Tsou MF (2013) Centriole distal appendages promote membrane docking, leading to cilia initiation. Genes Dev 27:163–168. doi:10.1101/gad.207043.112 [PubMed: 23348840]

196. Tian G, Lodowski KH, Lee R, Imanishi Y (2014) Retrograde intraciliary trafficking of opsin during the maintenance of cone-shaped photoreceptor outer segments of Xenopus laevis. J Comp Neurol 522:3577–3589. doi:10.1002/cne.23630 [PubMed: 24855015]

197. Tian G, Ropelewski P, Nemet I, Lee R, Lodowski KH, Imanishi Y (2014) An Unconventional Secretory Pathway Mediates the Cilia Targeting of Peripherin/rds. J Neurosci 34:992–1006. doi:10.1523/JNEUROSCI.3437-13.2014 34/3/992 [pii] [PubMed: 24431457]

198. Trivedi D, Colin E, Louie CM, Williams DS (2012) Live-cell imaging evidence for the ciliary transport of rod photoreceptor opsin by heterotrimeric kinesin-2. J Neurosci 32:10587–10593. doi:10.1523/JNEUROSCI.0015-12.2012 32/31/10587 [pii] [PubMed: 22855808]

199. Trojan P, Krauss N, Choe HW, Giessl A, Pulvermuller A, Wolfrum U (2008) Centrins in retinal photoreceptor cells: regulators in the connecting cilium. Prog Retin Eye Res 27:237–259. doi:10.1016/j.preteyeres.2008.01.003 [PubMed: 18329314]

200. Tsang SH, Sharma T (2018) Leber Congenital Amaurosis. Adv Exp Med Biol 1085:131–137. doi:10.1007/978-3-319-95046-4_26 [PubMed: 30578499]

201. Tsang WY, Bossard C, Khanna H, Peranen J, Swaroop A, Malhotra V, Dynlacht BD (2008) CP110 suppresses primary cilia formation through its interaction with CEP290, a protein deficient in human ciliary disease. Dev Cell 15:187–197. doi:10.1016/j.devcel.2008.07.004 [PubMed: 18694559]

202. Uzbekov R, Alieva I (2018) Who are you, subdistal appendages of centriole? Open Biol 8. doi:10.1098/rsob.180062

203. Vertii A, Hung HF, Hehnly H, Doxsey S (2016) Human basal body basics. Cilia 5:13. doi:10.1186/s13630-016-0030-8 [PubMed: 26981235]

204. Volland S, Hughes LC, Kong C, Burgess BL, Linberg KA, Luna G, Zhou ZH, Fisher SK, Williams DS (2015) Three-dimensional organization of nascent rod outer segment disk membranes. Proc Natl Acad Sci U S A 112:14870–14875. doi:10.1073/pnas.1516309112 [PubMed: 26578801]

205. Volland S, Williams DS (2018) Preservation of Photoreceptor Nanostructure for Electron Tomography Using Transcardiac Perfusion Followed by High-Pressure Freezing and Freeze-Substitution. Adv Exp Med Biol 1074:603–607. doi:10.1007/978-3-319-75402-4_73 [PubMed: 29721993]

206. Vuolo L, Stevenson NL, Heesom KJ, Stephens DJ (2018) Dynein-2 intermediate chains play crucial but distinct roles in primary cilia formation and function. Elife 7. doi:10.7554/eLife.39655

207. Wan W, Briggs JA (2016) Cryo-Electron Tomography and Subtomogram Averaging. Methods Enzymol 579:329–367. doi:10.1016/bs.mie.2016.04.014 [PubMed: 27572733]

208. Wang DY, Chan WM, Tam PO, Baum L, Lam DS, Chong KK, Fan BJ, Pang CP (2005) Gene mutations in retinitis pigmentosa and their clinical implications. Clin Chim Acta 351:5–16. doi:10.1016/j.cccn.2004.08.004 [PubMed: 15563868]

209. Wang J, Deretic D (2014) Molecular complexes that direct rhodopsin transport to primary cilia. Prog Retin Eye Res 38:1–19. doi:10.1016/j.preteyeres.2013.08.004 S1350-9462(13)00060-8 [pii] [PubMed: 24135424]

210. Wassie AT, Zhao Y, Boyden ES (2019) Expansion microscopy: principles and uses in biological research. Nat Methods 16:33–41. doi:10.1038/s41592-018-0219-4 [PubMed: 30573813]

211. Wei Q, Xu Q, Zhang Y, Li Y, Zhang Q, Hu Z, Harris PC, Torres VE, Ling K, Hu J (2013) Transition fibre protein FBF1 is required for the ciliary entry of assembled intraflagellar transport complexes. Nat Commun 4:2750. doi:10.1038/ncomms3750 [PubMed: 24231678]

212. Wensel TG (2012) Molecular Biology of Vision. In: Brady S (ed) Basic Neurochemistry, Principles of Molecular, Cellular, and Medical Neurobiology 8th ed. Elsevier, London,

213. Wensel TG, Gilliam JC (2015) Three-dimensional architecture of murine rod cilium revealed by cryo-EM. Methods Mol Biol 1271:267–292. doi:10.1007/978-1-4939-2330-4_18 [PubMed: 25697530]

214. Wensel TG, Zhang Z, Anastassov IA, Gilliam JC, He F, Schmid MF, Robichaux MA (2016) Structural and Molecular Bases of Rod Photoreceptor Morphogenesis and Disease. Progress in retinal and eye research 55:32–51. doi:10.1016/j.preteyeres.2016.06.002 [PubMed: 27352937]

215. Wensel TG, Zhang Z, Anastassov IA, Gilliam JC, He F, Schmid MF, Robichaux MA (2016) Structural and molecular bases of rod photoreceptor morphogenesis and disease. Prog Retin Eye Res 55:32–51. doi:10.1016/j.preteyeres.2016.06.002 [PubMed: 27352937]

216. Willig KI, Kellner RR, Medda R, Hein B, Jakobs S, Hell SW (2006) Nanoscale resolution in GFP-based microscopy. Nat Methods 3:721–723. doi:10.1038/nmeth922 [PubMed: 16896340]
217. Wolfrum U (1992) Cytoskeletal elements in arthropod sensilla and mammalian photoreceptors. Biol Cell 76:373–381 [PubMed: 1305480]
218. Yanagisawa H-a, Mathis G, Oda T, Hirono M, Richey EA, Ishikawa H, Marshall WF, Kikkawa M, Qin H (2014) FAP20 is an inner junction protein of doublet microtubules essential for both the planar asymmetrical waveform and stability of flagella in Chlamydomonas. Molecular biology of the cell 25:1472–1483. doi:10.1091/mbc.E13-08-0464 [PubMed: 24574454]
219. Yang J, Adamian M, Li T (2006) Rootletin interacts with C-Nap1 and may function as a physical linker between the pair of centrioles/basal bodies in cells. Mol Biol Cell 17:1033–1040. doi:E05-10-0943 [pii] 10.1091/mbc.E05-10-0943 [PubMed: 16339073]
220. Yang J, Gao J, Adamian M, Wen XH, Pawlyk B, Zhang L, Sanderson MJ, Zuo J, Makino CL, Li T (2005) The ciliary rootlet maintains long-term stability of sensory cilia. Mol Cell Biol 25:4129–4137. doi:25/10/4129 [pii] 10.1128/MCB.25.10.4129-4137.2005 [PubMed: 15870283]
221. Yang J, Li T (2005) The ciliary rootlet interacts with kinesin light chains and may provide a scaffold for kinesin-1 vesicular cargos. Exp Cell Res 309:379–389. doi:S0014-4827(05)00255-7 [pii] 10.1016/j.yexcr.2005.05.026 [PubMed: 16018997]
222. Yang J, Liu X, Yue G, Adamian M, Bulgakov O, Li T (2002) Rootletin, a novel coiled-coil protein, is a structural component of the ciliary rootlet. J Cell Biol 159:431–440. doi:10.1083/jcb.200207153 jcb.200207153 [pii] [PubMed: 12427867]
223. Yang J, Liu X, Zhao Y, Adamian M, Pawlyk B, Sun X, McMillan DR, Liberman MC, Li T (2010) Ablation of whirlin long isoform disrupts the USH2 protein complex and causes vision and hearing loss. PLoS Genet 6:e1000955. doi:10.1371/journal.pgen.1000955 [PubMed: 20502675]
224. Yang S, Bahl K, Chou HT, Woodsmith J, Stelzl U, Walz T, Nachury MV (2020) Near-atomic structures of the BBSome reveal the basis for BBSome activation and binding to GPCR cargoes. Elife 9. doi:10.7554/eLife.55954
225. Yang TT, Chong WM, Wang WJ, Mazo G, Tanos B, Chen Z, Tran TMN, Chen YD, Weng RR, Huang CE, Jane WN, Tsou MB, Liao JC (2018) Super-resolution architecture of mammalian centriole distal appendages reveals distinct blade and matrix functional components. Nat Commun 9:2023. doi:10.1038/s41467-018-04469-1 [PubMed: 29789620]
226. Yang TT, Su J, Wang WJ, Craige B, Witman GB, Tsou MF, Liao JC (2015) Superresolution Pattern Recognition Reveals the Architectural Map of the Ciliary Transition Zone. Sci Rep 5:14096. doi:10.1038/srep14096 [PubMed: 26365165]
227. Yang TT, Tran MNT, Chong WM, Huang CE, Liao JC (2019) Single-particle tracking localization microscopy reveals nonaxonemal dynamics of intraflagellar transport proteins at the base of mammalian primary cilia. Mol Biol Cell 30:828–837. doi:10.1091/mbc.E18-10-0654 [PubMed: 30759057]
228. Ye F, Nager AR, Nachury MV (2018) BBSome trains remove activated GPCRs from cilia by enabling passage through the transition zone. J Cell Biol 217:1847–1868. doi:10.1083/jcb.201709041 [PubMed: 29483145]
229. Ye X, Zeng H, Ning G, Reiter JF, Liu A (2014) C2cd3 is critical for centriolar distal appendage assembly and ciliary vesicle docking in mammals. Proc Natl Acad Sci U S A 111:2164–2169. doi:10.1073/pnas.1318737111 [PubMed: 24469809]
230. Young RW (1967) The renewal of photoreceptor cells outer segments The Journal of cell biology 33:61–72
231. Young RW (1971) The renewal of rod and cone outer segments in the rhesus monkey. J Cell Biol 49:303–318. doi:10.1083/jcb.49.2.303 [PubMed: 19866760]
232. Yu L, Li R, Zeng X, Wang H, Jin J, Yang G, Jiang R, Xu M (2020) Few Shot Domain Adaptation for in situ Macromolecule Structural Classification in Cryo-electron Tomograms. Bioinformatics. doi:10.1093/bioinformatics/btaa671
233. Yuodelis C, Hendrickson A (1986) A qualitative and quantitative analysis of the human fovea during development. Vision Res 26:847–855. doi:10.1016/0042-6989(86)90143-4 [PubMed: 3750868]

234. Zalenski AA, Majumder S, De K, Venere M (2020) An interphase pool of KIF11 localizes at the basal bodies of primary cilia and a reduction in KIF11 expression alters cilia dynamics. Sci Rep 10:13946. doi:10.1038/s41598-020-70787-4 [PubMed: 32811879]

235. Zhang P (2019) Advances in cryo-electron tomography and subtomogram averaging and classification. Curr Opin Struct Biol 58:249–258. doi:10.1016/j.sbi.2019.05.021 [PubMed: 31280905]

236. Zhang Q, Yu D, Seo S, Stone EM, Sheffield VC (2012) Intrinsic protein-protein interaction-mediated and chaperonin-assisted sequential assembly of stable bardet-biedl syndrome protein complex, the BBSome. J Biol Chem 287:20625–20635. doi:10.1074/jbc.M112.341487 [PubMed: 22500027]

237. Zhao Y, Hong DH, Pawlyk B, Yue G, Adamian M, Grynberg M, Godzik A, Li T (2003) The retinitis pigmentosa GTPase regulator (RPGR)-interacting protein: subserving RPGR function and participating in disk morphogenesis. Proc Natl Acad Sci U S A 100:3965–3970. doi:10.1073/pnas.0637349100 0637349100 [pii] [PubMed: 12651948]

238. Zwettler FU, Reinhard S, Gambarotto D, Bell TDM, Hamel V, Guichard P, Sauer M (2020) Molecular resolution imaging by post-labeling expansion single-molecule localization microscopy (Ex-SMLM). Nat Commun 11:3388. doi:10.1038/s41467-020-17086-8 [PubMed: 32636396]

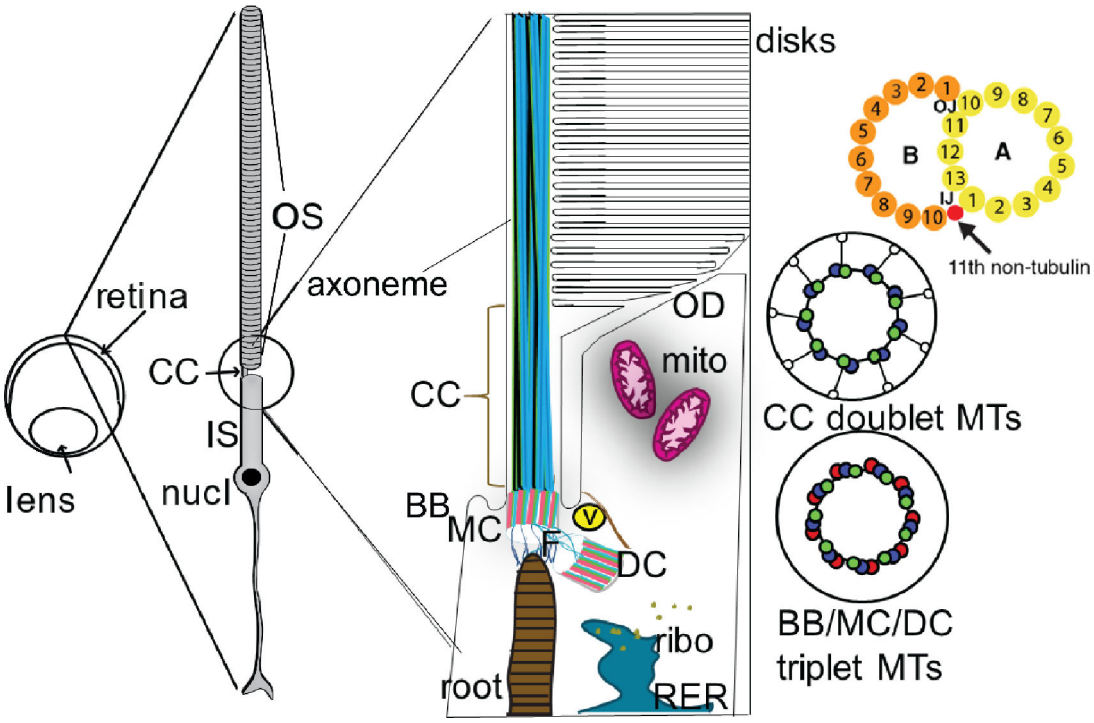

Fig. 1.

Schematic depiction of the photoreceptor (rod) sensory cilium. The ciliary structures of a rod sensory cilium and adjacent cellular structures are depicted roughly to scale, based on an outer segment length of approximately 20 μm and a connecting cilium diameter of ~300 nm. The cross-sectional views of the microtubule bundles to the right are at a different scale, based on the same 300 nm diameter. The cartoon of an individual doublet microtubule doublet at the upper right has a scale corresponding to a diameter of the A-microtubule of ~22 nm. OS, outer segment; CC, connecting cilium; MTs, microtubules; BB, basal body; MC mother centriole; DC, daughter centriole; root, ciliary rootlet; ribo, ribosomes; RER, rough endoplasmic reticulum; V, vesicle (representing the large number of vesicles of varying size typically observed in this region); F, fibrils connecting the rootlet to the basal body; mito, mitochondria (much more elongated in rods than depicted here); OD, open discs at the base of the outer segment, with membranes continuous with the plasma membrane. To the right are cross-sectional views of the 9-fold symmetric arrangement of the MT bundles in the centrioles and CC. One of these doublet microtubules is further zoomed in to display the protofilament structure of the A- and B-tubules. Above the basal discs, the discs extend to a diameter in most mammals of ~1.4 μm. Not depicted are the dense networks of fibers and associated vesicles constituting the pericentriolar material, and present at varying densities throughout the distal inner segment, the bundles of actin filaments at the base of the outer segment, or the connections between the open basal discs and the adjacent membrane of the periciliary inner segment membrane. The ciliary pocket is depicted at either side of the CC.

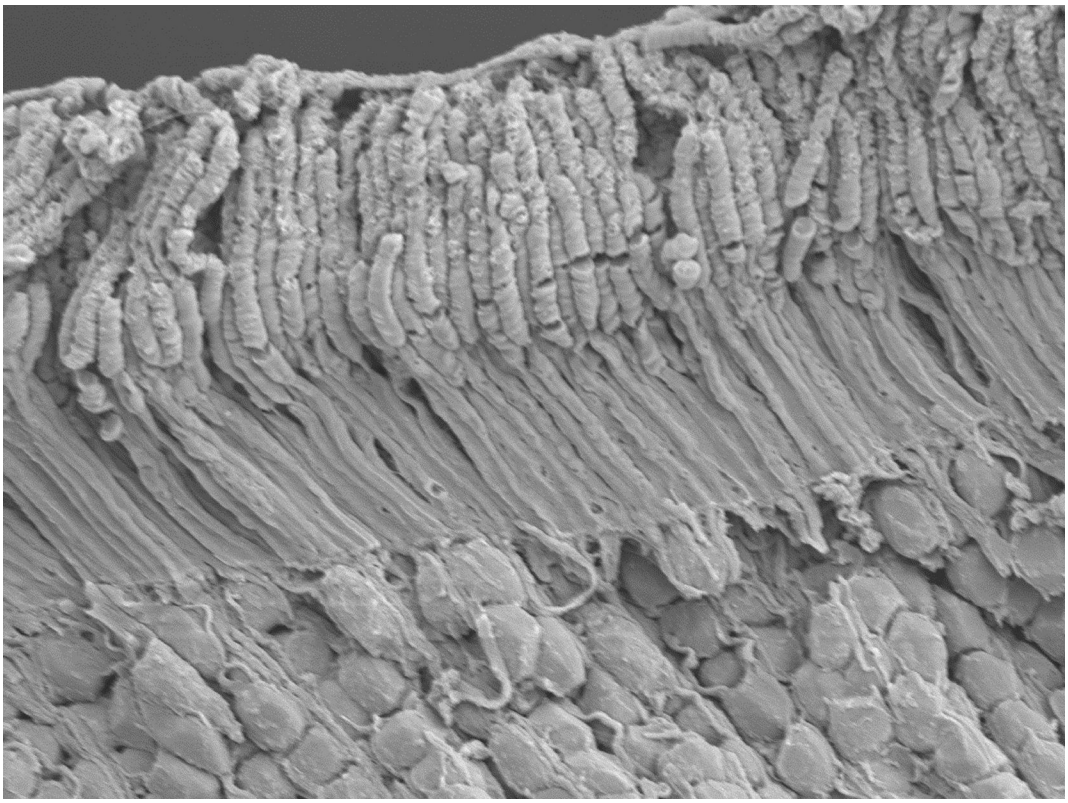

Fig. 2.
Scanning electron microscope (SEM) of the outer portion of a mouse retina showing outer segments, inner segments and some nuclei. Reproduced from ref. [212]

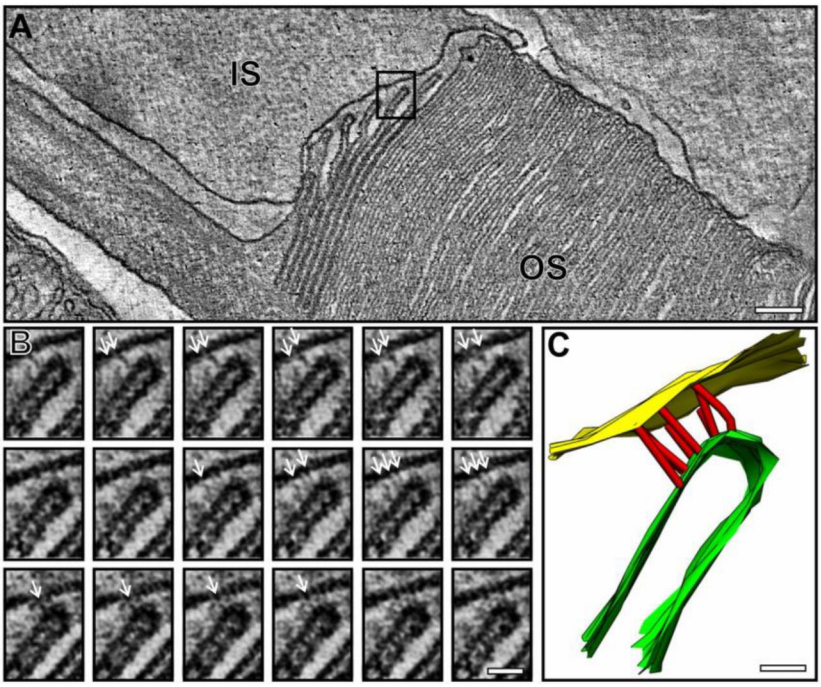

Fig. 3.

Reconstruction of base of rod outer segment from electron tomography of serial sections of fixed and stained mouse retina. Inset B shows a series of slices through the tomographic map at different z positions. Inset C shows a close-up of a segmented portion of the tomogram showing attachments between the rim of a basal disc and the adjacent inner segment plasma membrane. Reproduced from ref. 18

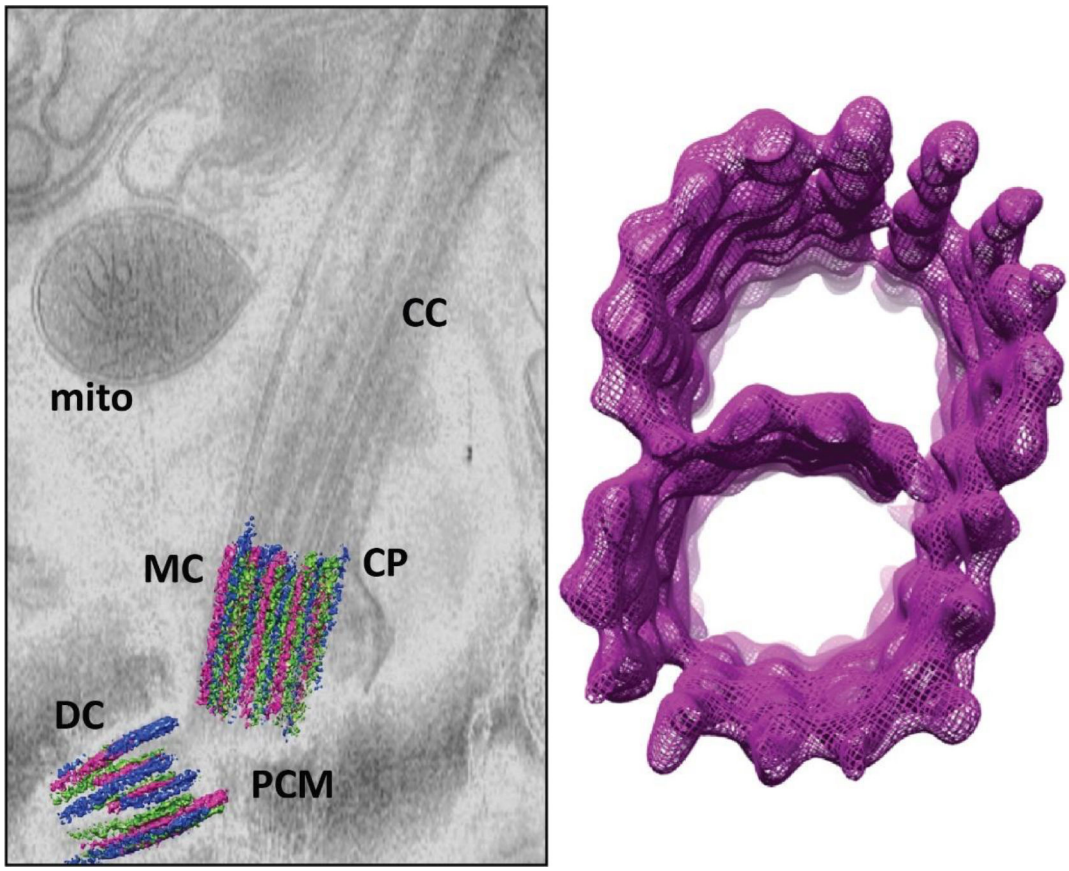

Fig. 4.

Cryo-electron tomography of the base of the rod sensory cilium. Left panel shows a slice from a tomogram of a mouse rod embedded in vitreous ice, with the triplet microtubules of the basal body centriole pair segmented in magenta, green and blue surfaces for a, b and c MT. Right panel shows a map of a 72 nm (9 tubulin dimer repeats) section of a microtubule doublet generated by subtomogram averaging of doublets in connecting cilia. Tomograms were generated as described [157] and subtomogram averaging carried out as in [32]. CC, connecting cilium; MC, mother centriole; DC, daughter centriole; PCM, pericentriolar material/matrix; CP, ciliary pocket membrane; mito, mitochondrion

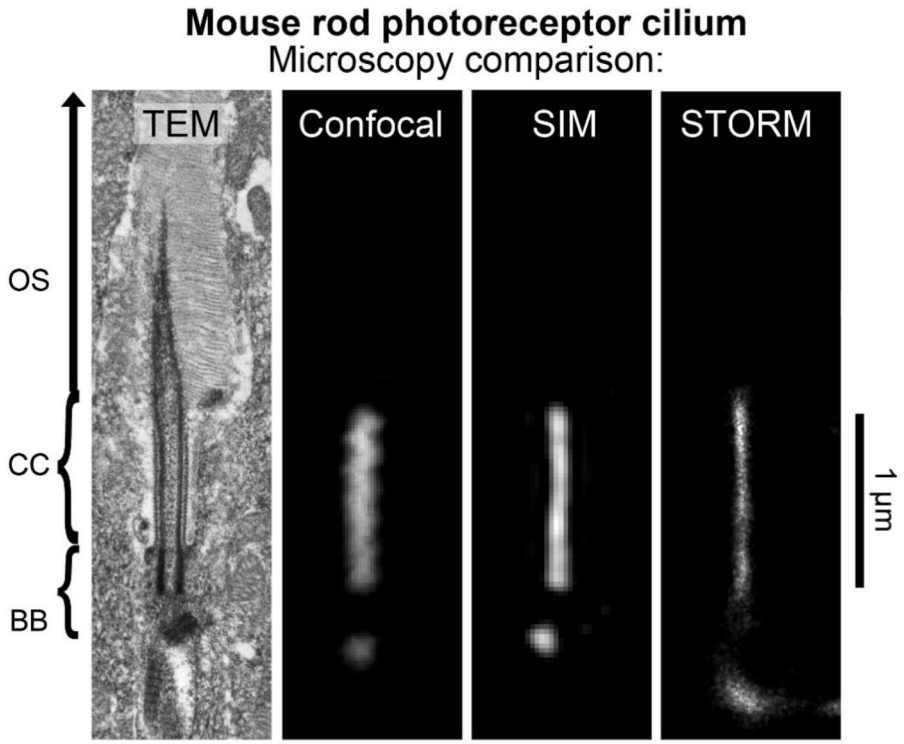

Figure 5.

The mouse rod photoreceptor cilium as imaged with alternative microscopies. Examples of an isolated rod photoreceptor cilia from mouse retina tissue samples are compared at the same scale from images captured by transmission electron microscopy (TEM), and by the fluorescence microscopies: confocal microscopy, structured illumination microscopy (SIM), and stochastic optical reconstruction microscopy (STORM). SIM and STORM are super-resolution fluorescence microscopies with optimal X-Y lateral resolutions of approximately 100 nm and 20 nm, respectively [66], [72]. Mouse retina samples imaged with fluorescence microscopy were immunostained with a pan-centrin antibody, which targets the lumen of the connecting cilium (CC) axoneme and the centrioles of the basal body (BB) in rods

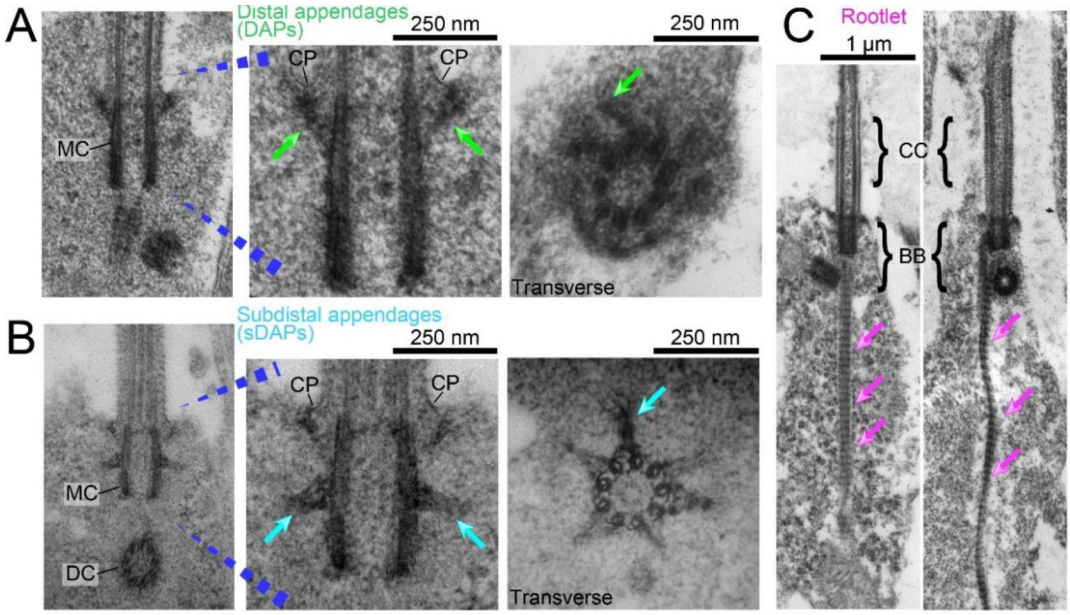

Fig. 6.

Transmission electron microscopy (TEM) of mouse rod sensory cilia, highlighting A, distal appendages, green arrows, B, subdistal appendages, cyan arrows or C, ciliary rootlet, magenta arrows. MC, mother centriole; DC, daughter centriole; CC, connecting cilium, BB, basal body; CP, ciliary pocket. Samples in A and B were prepared and imaged as described [157]. (A) In TEM images of the BB region from age P14 mouse rod photoreceptors, the distal appendages are electron dense projections attached to the distal end of the mother centriole that apparently connect to the plasma membrane directly beneath the connecting cilium. In the transverse orientation, the DAP “blades” (green arrows) extend radially from each MC triplet. (B) In TEM examples of the BB in P7 mouse rod neurons, the subdistal appendages (sDAPs, cyan arrows) are attached the MC proximal the DAPs. The daughter centriole (DC) is located beneath the MC in this rod BB. In the transverse orientation, 6 triangular sDAPs are each linked to 2 adjacent MC triplets and extend radially into the inner segment cytoplasm. (C) In TEM examples of rods from adult mouse retinas that were mildly permeabilized with Triton X-100, the striated rootlet (magenta arrows) can be seen linked to the BB centrioles and extending through the inner segment cytoplasm.

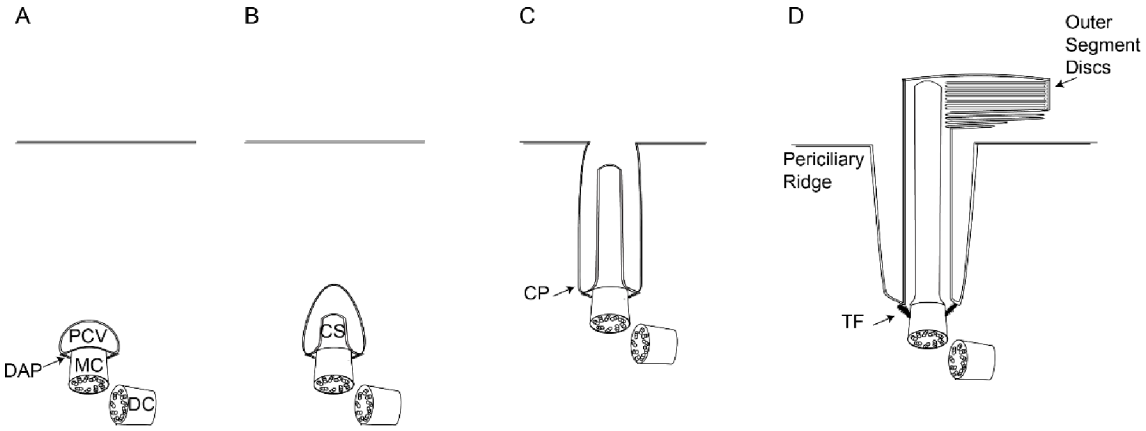

Fig. 7.

Schematic of intracellular ciliogenesis. A, primary ciliary vesicle docks to the distal end of the mother centriole. B, ciliary shaft extends within the ciliary vesicle. C, the ciliary vesicle and plasma membrane fuse to expose the cilium outside the cell. D, outer segment discs form and mature. DAP, distal appendage; PCV, primary ciliary vesicle; MC, mother centriole; DC, daughter centriole; CS, ciliary shaft; CP, ciliary pocket; TF, transition fibers

Table 1.

Summary of current methodologies for microscopic imaging of photoreceptor neurons.

		Examples of these methods used in photoreceptors
Superresolution Fluorescence	• SIM • STED • Expansion Microscopy	• SIM [105,181] (https://www.biorxiv.org/content/10.1101/2020.10.28.357806v1)
Superresolution Single Molecule Fluorescence	• STORM • PALM • DNA-PAINT	• [41,157]
Electron Microscopy	• Transmission EM • Scanning EM • Cryo – Electron Tomography	• Conventional TEM [17,19,23,25–29,42,64,71,95,145,170,169,175,182,185,204,217,5,7] • Freeze-fracture SEM [159,160,158] • Focused ion beam SEM [142] • Cryo-ET [41,58,138,157,19,204]

Table 2.

Summary of ciliary sub-structures in photoreceptor neurons.

Ciliary structure	Location in photoreceptors	Protein marker	Reference
Basal Body (BB)	Inner Segment	Centrin	[170,199,157]
Distal Appendages (DAPs)	Inner Segment	CEP164, CEP89/CCDC123, CEP83/CCDC41, SCLT1, FBF1	[195,225]
Subdistal Appendages (sDAPs)	Inner Segment	ODF2, CEP128, centriolin, ninein, CEP170	[33]
Pericentriolar Material	Inner Segment	CEP135, ninein, pericentrin, C-Nap-1/Cep250, gamma tubulin	[81,143,219,124,234,126]
Centriolar Satellites	Inner Segment	PCM1, AZI/Cep131, SSX2IP, CP110	[70,124,45,30,201,94]
Periciliary Membrane Complex (PMC)	Inner Segment	Myosin VIIa, VLGR1, whirlin	[111,223,157]
Ciliary Rootlet	Inner Segment/Outer Nuclear Layer	Rootletin, C-Nap-1/Cep250	[118,221,219]
Ciliary Necklace/Y-links	Connecting Cilium	CEP290 (in *Chlamydomonas* flagella)	[39]
Axoneme	Outer Segment	RP1, MAK	[123]